Commun. Comput. Phys.
doi: 10.4208/cicp.OA-2022-0269

Vol. **37**, No. 1, pp. 137-170
January 2025

Second-Order Linear Stabilized Semi-Implicit Crank-Nicolson Scheme for the Cahn-Hilliard Model with Dynamic Boundary Conditions

Xiangjun Meng[1,2], Xuelian Bao[3,1] and Zhengru Zhang[1,*]

[1] *School of Mathematical Sciences, Beijing Normal University, Beijing 100875, China.*
[2] *School of Physical and Mathematical Sciences, Nanyang Technological University, 639798, Singapore.*
[3] *School of Mathematics, South China University of Technology, Guangzhou, Guangdong 510641, China.*

Communicated by Axel Voigt

Received 24 October 2022; Accepted (in revised version) 4 July 2023

Abstract. We propose a kind of second-order stabilized Crank-Nicolson scheme which can be applied to three types of Cahn-Hilliard model with dynamic boundary conditions. We give the corresponding proof of stability and convergence theoretically which takes the reaction rate dependent dynamic boundary conditions as an example. We verify the effectiveness and universality of our proposed scheme by conducting some typical numerical simulations and comparing with the literature works. It's found that second-order scheme takes much less CPU time than the first-order scheme to reach the same final time.

AMS subject classifications: 65M12, 65N12, 65Z05

Key words: Cahn-Hilliard equation, dynamic boundary conditions, reaction rate, second-order Crank-Nicolson formula, energy stability, convergence analysis.

1 Introduction

As pointed out in [33], the evolution range of Cahn-Hilliard equation is quite wide which can describe the important qualitative characteristics of many systems undergoing phase separation at different time stages, such as the phase separation, the process of nucleation, coarsening in heterogeneous systems [4, 5, 33] and extension of coupling classical

*Corresponding author. *Email addresses:* `xjmengbnu@163.com` (X. Meng), `baoxuelian@scut.edu.cn` (X. Bao), `zrzhang@bnu.edu.cn` (Z. Zhang)

phase-field model with magnetic field [1,53]. Cahn-Hilliard equation is a representative of the so-called diffusion interface model which describes the evolution of free interface during phase transition [44]. Different from the classical sharp-interface formulation, this approach has several advantages. For instance, it can avoid evolution of complex geometries and topological changes of the interface [12], and explicit tracking of the interface.

The standard Cahn-Hilliard equation can be written as follows,

$$\begin{cases} \phi_t = \Delta\mu, & (\mathbf{x},t)\in\Omega\times(0,T), \\ \mu = -\varepsilon\Delta\phi + \dfrac{1}{\varepsilon}F'(\phi), & (\mathbf{x},t)\in\Omega\times(0,T), \end{cases} \tag{1.1}$$

where μ denotes the chemical potential, the parameter $\varepsilon>0$ means the thickness of the interface and $\Omega\subseteq\mathbb{R}^d$ $(d=2,3)$ denotes a bounded domain whose boundary $\Gamma=\partial\Omega$ with the unit outward normal vector $\mathbf{n}$. The function ϕ has different interpretations depending on the physical environment, such as volume fraction, mass fraction or mole fraction [12,33]. In general, it represents the concentration of two components by rescaling, therefore the value of ϕ shall be taken in the physical interval $[-1,1]$ with the $\phi=\pm1$ corresponding to the pure phase of the materials, which are separated by an interfacial region whose thickness is proportional to ε.

The Cahn-Hilliard equation can be alternatively viewed as the gradient flow of the Ginzburg-Landau type energy functional

$$E^{bulk}(\phi) = \int_\Omega \left\{ \frac{\varepsilon}{2}|\nabla\phi|^2 + \frac{1}{\varepsilon}F(\phi) \right\} dx,$$

in H^{-1}. The energy functional E^{bulk} consists of two parts: the hydrophilic (gradient term) and hydrophobic (double-well term) tendency of the phase-field variable ϕ. $F(x)$ is a given double-well potential and $f(x)=F'(x)$ as below

$$F(x)=\frac{1}{4}(x^2-1)^2, \quad f(x)=x^3-x, \quad x\in\mathbb{R}. \tag{1.2}$$

Since (1.1) is a fourth order parabolic equation for variable ϕ, suitable initial and boundary conditions should be taken to form a well-posed problem. The classical setting is homogeneous Neumann condition:

$$\begin{cases} \partial_{\mathbf{n}}\mu = 0, & (\mathbf{x},t)\in\Gamma\times(0,T), \\ \partial_{\mathbf{n}}\phi = 0, & (\mathbf{x},t)\in\Gamma\times(0,T), \end{cases}$$

where $\partial_{\mathbf{n}}$ represents the outward normal derivative on Γ. The energetic variational approach reveals that the Cahn–Hilliard equation together with the classical boundary conditions naturally fulfills two important physical constraints, the mass conservation

$$\int_\Omega \phi(t)dx = \int_\Omega \phi(0)dx, \quad \forall t\in[0,T],$$

and energy dissipation

$$\frac{d}{dt}E^{bulk}(\phi)=-\|\nabla\mu\|_{\Omega}^{2}\leq 0.$$

The influence of boundary (solid wall) on the phase separation process of binary mixtures has attracted extensive attention of scientists. For example, the structure of binary polymer mixture during phase separation may be frozen by rapid quenching into the glassy state, and micro-structure on small length scale can be generated on the surface [14]. However, the standard homogeneous Neumann condition ignores the influence of boundary on volume dynamics. In order to describe the short-range interaction between the two components of the wall and the mixture, a suitable surface free energy functional should be introduced into the system

$$E^{total}(\phi,\psi)=E^{bulk}(\phi)+E^{surf}(\psi), \tag{1.3}$$

with

$$E^{surf}(\psi)=\int_{\Gamma}\left\{\frac{\delta\kappa}{2}|\nabla_{\Gamma}\psi|^{2}+\frac{1}{\delta}G(\psi)\right\}dS, \tag{1.4}$$

where δ denotes the thickness of the interface area on the boundary and the parameter κ is related to the surface diffusion. If $\kappa=0$, it is related to the moving contact line problem [24]. G is the surface potential, ∇_Γ represents the tangential surface gradient operator and Δ_Γ denotes the Laplace-Beltrami operator on Γ. Like the classical periodic Neumann boundary conditions, the Cahn-Hilliard equation for the phase separation process with boundary effects still needs to be supplemented by two boundary conditions, and is required from mass conservation and energy dissipation. However, the difference is that nontrivial boundary effects driven by surface energy (1.4) must be involved [9, 11, 16, 26–28, 32, 34, 48]. In this paper, the following three types of dynamic boundary conditions are considered.

Recently, Knopf, Lam, Liu and Metzger proposed a new type of dynamic boundary conditions [27] as follows,

$$\begin{cases}\phi|_{\Gamma}=\psi, & (\mathbf{x},t)\in\Gamma\times(0,T),\\ K\partial_{\mathbf{n}}\mu=\mu_{\Gamma}-\mu, & (\mathbf{x},t)\in\Gamma\times(0,T),\\ \psi_t=\Delta_{\Gamma}\mu_{\Gamma}-\partial_{\mathbf{n}}\mu, & (\mathbf{x},t)\in\Gamma\times(0,T),\\ \mu_{\Gamma}=-\delta\kappa\Delta_{\Gamma}\psi+\frac{1}{\delta}G'(\psi)+\varepsilon\partial_{\mathbf{n}}\phi, & (\mathbf{x},t)\in\Gamma\times(0,T),\end{cases} \tag{1.5}$$

referred to the boundary conditions of KLLM model as in [3]. Here, μ, μ_Γ denote the chemical potentials in the bulk and on the boundary, respectively. The equation on the boundary can be viewed as a chemical reaction in a general case since it describes that one species (ϕ) changes into another species (ψ) on the boundary. So it is also called Cahn–Hilliard equation with reaction rate dependent dynamic boundary conditions. The Robin type boundary condition indicates that the mass flux $\partial_{\mathbf{n}}\mu$ is driven by differences in the chemical potentials, where K is a positive parameter describing the extent of mass exchange. This model fulfills the conservation of total mass

$$\int_\Omega \phi(t)dx+\int_\Gamma \psi(t)dS=\int_\Omega \phi(0)dx+\int_\Gamma \psi(0)dS, \quad \forall t\in[0,T],$$

and dissipation of the total free energy

$$\frac{d}{dt}E^{total}(\phi,\psi)=-\|\nabla\mu\|_\Omega^2-\|\nabla_\Gamma\mu_\Gamma\|_\Gamma^2-K\|\partial_{\mathbf{n}}\mu\|_\Gamma^2\le 0.$$

There is no need to impose any boundary conditions on ψ and μ_Γ, since the boundary Γ is assumed to be a closed manifold. The authors have proved the existence, uniqueness and regularity of weak solutions [27] and investigated long-time behavior [18]. They also investigated the asymptotic limits as $K\to 0^+$ and $K\to\infty$, establishing convergence rates for these limits.

Here, the dynamic boundary conditions of the case $K\to 0^+$ is

$$\begin{cases} \phi|_\Gamma=\psi, & (\mathbf{x},t)\in\Gamma\times(0,T),\\ \psi_t=\Delta_\Gamma\mu-\partial_{\mathbf{n}}\mu, & (\mathbf{x},t)\in\Gamma\times(0,T),\\ \mu=-\delta\kappa\Delta_\Gamma\psi+\frac{1}{\delta}G'(\psi)+\varepsilon\partial_{\mathbf{n}}\phi, & (\mathbf{x},t)\in\Gamma\times(0,T), \end{cases} \tag{1.6}$$

which was proposed by Goldstein, Miranville and Schimperna in [19]. We also use the authors' initials and refer it to be the boundary conditions of GMS model for convenience. Different from the KLLM model, the chemical potential on the boundary μ_Γ is equal to potential in the bulk μ in GMS model. It also required that the total mass is conserved and the total free energy decreases with time,

$$\int_\Omega \phi(t)dx+\int_\Gamma \psi(t)dS=\int_\Omega \phi(0)dx+\int_\Gamma \psi(0)dS, \quad \forall t\in[0,T].$$

and

$$\frac{d}{dt}E^{total}(\phi,\psi)=-\|\nabla\mu\|_\Omega^2-\|\nabla_\Gamma\mu_\Gamma\|_\Gamma^2\le 0.$$

The existence, uniqueness and regularity of global weak solutions are proved, and their long-term behaviors are studied, including the existence of a compact global attractor and convergence to a single equilibrium as $t\to\infty$ [19].

And the dynamic boundary conditions of the case $K\to\infty$ is

$$\begin{cases} \phi|_\Gamma=\psi, & (\mathbf{x},t)\in\Gamma\times(0,T),\\ \partial_{\mathbf{n}}\mu=0, & (\mathbf{x},t)\in\Gamma\times(0,T),\\ \psi_t=\Delta_\Gamma\mu_\Gamma, & (\mathbf{x},t)\in\Gamma\times(0,T),\\ \mu_\Gamma=-\delta\kappa\Delta_\Gamma\psi+\frac{1}{\delta}G'(\psi)+\varepsilon\partial_{\mathbf{n}}\phi, & (\mathbf{x},t)\in\Gamma\times(0,T), \end{cases} \tag{1.7}$$

which was proposed by Liu and Wu, called Liu-Wu model [28]. It is worth noting that the condition $\partial_{\mathbf{n}}\mu=0$ assumes that there is no mass exchange between the bulk and the boundary, which is different from KLLM model and GMS model. So KLLM model (1.5) can be interpreted as an interpolation between GMS model (1.6) and Liu-Wu model (1.7), see [27] for detailed discussions. So except for the dissipation of the total free energy and total mass is conserved, it has the conservation of mass both in the bulk Ω and on the boundary Γ respectively,

$$\int_\Omega \phi(t)dx=\int_\Omega \phi(0)dx, \quad \int_\Gamma \psi(t)dS=\int_\Gamma \psi(0)dS, \quad \forall t\in[0,T].$$

Well-posedness of problem (1.7) was first analyzed in [28] when F and G are suitable regular potentials (including the typical choice like (1.2) for F and G). They obtained the existence of global weak (and strong) solutions by finding the convergent subsequence of the approximate solution after passing to the limit (See [28], Theorem 3.1). Well-posedness of problem (1.7) with singular potentials was also established in [10]. The existence and uniqueness of global weak solutions as well as strong solution were proved.

There are many effective numerical methods for Cahn-Hilliard equation. For time discretization, the convex splitting method [21, 35], the invariant energy quadratization (IEQ) method [38,41,46,47,49,50,52–54], the scalar auxiliary variable (SAV) method [36], the exponential time difference (ETD) scheme [25], the Runge-Kutta scheme [22, 39], the stabilized linearly implicit approach and adaptive BDF2 implicit time-stepping method [31] are developed recently. Researchers have constructed different numerical schemes by adding different stabilizers [6, 23, 30, 37]. This idea has been adopted in [13] for the stabilized Crank-Nicolson schemes for phase field models. Wu et al. [45] proposed another stabilized second-order Crank-Nicolson scheme for tumor-growth system, which involved a new concave-convex energy splitting. These time marching schemes will lead to a linear system, which is easier to solve than the nonlinear system generated by the traditional convex splitting scheme with implicitly dealing with the nonlinear convex force.

Recently, various numerical approximations for the Cahn-Hilliard equation with dynamic boundary conditions have been studied (see [3,7,8,15,20,40]). Specifically, a finite element approach for the Liu-Wu model has been proposed in [17,40], where the model is simulated by the direct discretization based on piecewise linear finite element, and the corresponding nonlinear system is solved by the Newton's method. A linear first-order energy stable numerical scheme for Liu-Wu model and KLLM model has been proposed, which is an extension of the stable linear implicit method for the classical boundary conditions [2,3]. Meng and Bao et al. [29] extended the first-order scheme to the second-order scheme for Liu-Wu model (1.7), where the time is discretized by BDF2 scheme.

In this paper, inspired by [3], we focus on the second-order Crank-Nicolson schemes for the above three models (1.5), (1.6) and (1.7). The stability and convergence of second-order semi-implicit time marching schemes are studied. In order to approximate the nonlinear term with second-order accuracy, the explicit extrapolation method is used and stabilizers are added to ensure energy dissipation, where the stabilizers are inspired by the work [42] and [43] by Wang and Yu, namely, SL-CN and SL-BDF2. The main features of our scheme include the following:

(1) We propose the stabilized Crank-Nicolson scheme for three types of Cahn-Hilliard model with dynamic boundary conditions;

(2) For KLLM model, to the best of our knowledge, this is the first linear, second-order stabilized semi-implicit scheme;

(3) At the discrete level, the constant coefficient linear systems are produced, then we only need to solve the linear equation at each step, which reduces the computation cost greatly;

(4) Discrete energy dissipation and error analysis are proved in detail for KLLM model (1.5);

(5) For the Cahn-Hilliard model with dynamic boundary conditions, we are the first to compare the second-order scheme with the first-order scheme, which verifies the efficiency of the second-order scheme.

The rest of this article is organized as follows. We first introduce some definitions and notations in Section 2. In Section 3, we present second-order Crank-Nicolson schemes of KLLM model. The stability of corresponding modified energy is given after the proposed scheme. Subsequently, the convergence estimate of KLLM model (1.5) is provided in Section 4. In Section 5, we present some numerical experiments, including the accuracy test about time t, the droplet model with different types of dynamic boundary conditions and cases with different potential functions, validating the second-order scheme and conducting comparisons between the second-order and first-order scheme. Finally, the concluding remarks are given in Section 6.

2 Preliminaries

Before giving the stabilized scheme and corresponding error analysis, we make some definitions in this section which will be used in the paper.

We consider a finite time interval $[0,T]$ and a domain $\Omega \subseteq \mathbb{R}^d$, which is a bounded domain with sufficient smooth boundary $\Gamma = \partial\Omega$ and $\mathbf{n} = \mathbf{n}(x)$ is the unit outward normal vector on Γ.

We use $\|\cdot\|_{m,p,\Omega}$ to denote the standard norm of the Sobolev space $W^{m,p}(\Omega)$ and $\|\cdot\|_{m,p,\Gamma}$ to denote the standard norm of the Sobolev space $W^{m,p}(\Gamma)$. In particular, we use $\|\cdot\|_{L^p(\Omega)}$, $\|\cdot\|_{L^p(\Gamma)}$ to denote the norm of $W^{0,p}(\Omega) = L^p(\Omega)$ and $W^{0,p}(\Gamma) = L^p(\Gamma)$; $\|\cdot\|_{m,\Omega}$, $\|\cdot\|_{m,\Gamma}$ to denote the norm of $W^{m,2}(\Omega) = H^m(\Omega)$ and $W^{m,2}(\Gamma) = H^m(\Gamma)$; we also use $\|\cdot\|_\Omega$ and $\|\cdot\|_\Gamma$ to denote the norm of $W^{0,2}(\Omega) = L^2(\Omega)$ and $W^{0,2}(\Gamma) = L^2(\Gamma)$. Let $(\cdot,\cdot)_\Omega$, $(\cdot,\cdot)_\Gamma$ represent the inner product of $L^2(\Omega)$ and $L^2(\Gamma)$, respectively.

Let τ be the time step size. For a sequence of functions f^0, $f^1,\cdots,f^N$ in some Hilbert space E, we denote the sequence by $\{f_\tau\}$ and define the following discrete norm for $\{f_\tau\}$,

$$\|f_\tau\|_{l^\infty(E)}=\max_{0\le n\le N}\Big(\|f^n\|_E\Big).$$

We denote by C a general constant which is independent of τ but possibly depends on the parameters and solutions, and use $f\lesssim g$ to say that there is a general constant C such that $f\le Cg$.

For simplicity, we denote

$$\begin{aligned}&\delta_t\phi^{n+1}:=\phi^{n+1}-\phi^n,\quad \delta_{tt}\phi^{n+1}:=\phi^{n+1}-2\phi^n+\phi^{n-1},\quad \hat{\phi}^{n+\frac12}=\frac32\phi^n-\frac12\phi^{n-1},\\ &\delta_t\psi^{n+1}:=\psi^{n+1}-\psi^n,\quad \delta_{tt}\psi^{n+1}:=\psi^{n+1}-2\psi^n+\psi^{n-1},\quad \hat{\psi}^{n+\frac12}=\frac32\psi^n-\frac12\psi^{n-1}.\end{aligned}$$

3 Second-order scheme for KLLM model

In this section, we propose the stabilized linear Crank-Nicolson scheme (SL-CN) for KLLM model. The surface diffusion term is treated implicitly, while the nonlinear chemical potential is approximated by a second-order explicit extrapolation formula. In particular, $f=F',g=G'$ are the derivatives of nonlinear chemical potentials. We notice that a second-order approximation to f and g at time step t^{n+1} are taken in the form $f(\frac32\phi^n-\frac12\phi^{n-1})$ and $g(\frac32\psi^n-\frac12\psi^{n-1})$. T is the fixed time, N is the number of time steps and $\tau=T/N$ is the step size. Five second-order accurate regularization terms, such as $A\tau\Delta\left(\phi^{n+1}-\phi^n\right)$, $A\tau\Delta_\Gamma\left(\psi^{n+1}-\psi^n\right)$, $B_1\left(\phi^{n+1}-2\phi^n+\phi^{n-1}\right)$, $B_2\left(\psi^{n+1}-2\psi^n+\psi^{n-1}\right)$ and $A\tau\partial_{\mathbf{n}}\left(\phi^{n+1}-\phi^n\right)$ are added to the bulk equation and boundary equation to enhance the energy stability at a theoretical level.

Below we will establish the energy stability for the second-order scheme with an assumption given in advance.

Assumption 1. Assume that the Lipschitz properties hold for the second derivative of F with respect to ϕ and the second derivative of G with respect to ψ (namely, f' and g'). f' and g' are bounded. Precisely, there exists positive constants K_1, K_2, L_1 and L_2 such that

$$|f'(\phi_1)-f'(\phi_2)|\le K_1|\phi_1-\phi_2|,\quad |g'(\psi_1)-g'(\psi_2)|\le K_2|\psi_1-\psi_2|,\quad \forall\phi_1,\phi_2,\psi_1,\psi_2\in\mathbb{R},$$

and

$$\max_{\phi\in\mathbb{R}}|f'(\phi)|\le L_1,\quad \max_{\psi\in\mathbb{R}}|g'(\psi)|\le L_2.$$

We propose a SL-CN scheme for the KLLM model as follows,

$$\begin{cases} \dfrac{\phi^{n+1}-\phi^n}{\tau}=\Delta\mu^{n+\frac{1}{2}}, & \mathbf{x}\in\Omega, \quad (3.1)\\ \mu^{n+\frac{1}{2}}=-\varepsilon\Delta\left(\dfrac{\phi^{n+1}+\phi^n}{2}\right)+\dfrac{1}{\varepsilon}f\left(\dfrac{3}{2}\phi^n-\dfrac{1}{2}\phi^{n-1}\right) & \\ \qquad -A\tau\Delta\left(\phi^{n+1}-\phi^n\right)+B_1\left(\phi^{n+1}-2\phi^n+\phi^{n-1}\right), & \mathbf{x}\in\Omega, \quad (3.2)\\ K\partial_{\mathbf{n}}\mu^{n+\frac{1}{2}}=\mu_\Gamma^{n+\frac{1}{2}}-\mu^{n+\frac{1}{2}}, & \mathbf{x}\in\Gamma, \quad (3.3)\\ \phi^{n+1}|_\Gamma=\psi^{n+1}, & \mathbf{x}\in\Gamma, \quad (3.4)\\ \dfrac{\psi^{n+1}-\psi^n}{\tau}=\Delta_\Gamma\mu_\Gamma^{n+\frac{1}{2}}-\partial_{\mathbf{n}}\mu^{n+\frac{1}{2}}, & \mathbf{x}\in\Gamma, \quad (3.5)\\ \mu_\Gamma^{n+\frac{1}{2}}=-\delta\kappa\Delta_\Gamma\left(\dfrac{\psi^{n+1}+\psi^n}{2}\right)+\dfrac{1}{\delta}g\left(\dfrac{3}{2}\psi^n-\dfrac{1}{2}\psi^{n-1}\right)+\varepsilon\partial_{\mathbf{n}}\left(\dfrac{\phi^{n+1}+\phi^n}{2}\right) & \\ \qquad -A\tau\Delta_\Gamma\left(\psi^{n+1}-\psi^n\right)+B_2\left(\psi^{n+1}-2\psi^n+\psi^{n-1}\right)+A\tau\partial_{\mathbf{n}}\left(\phi^{n+1}-\phi^n\right), & \mathbf{x}\in\Gamma. \quad (3.6) \end{cases}$$

The energy stability is as follows.

Theorem 3.1. *Assume that Assumption* 1 *holds, then under the conditions*

$$A\geq\max\left\{\frac{L_1^2}{16\varepsilon^2},\frac{L_2^2}{16\delta^2}\right\}, \tag{3.7}$$

$$B_1\geq\frac{L_1}{2\varepsilon}, \quad B_2\geq\frac{L_2}{2\delta}, \tag{3.8}$$

we have

$$\begin{aligned} &\tilde{E}(\phi^{n+1},\psi^{n+1})\\ \leq&\tilde{E}(\phi^n,\psi^n)-\left(2\sqrt{A}-\frac{L_1}{2\varepsilon}\right)\|\delta_t\phi^{n+1}\|_\Omega^2-\left(2\sqrt{A}-\frac{L_2}{2\delta}\right)\|\delta_t\psi^{n+1}\|_\Gamma^2\\ &-\left(\frac{B_1}{2}-\frac{L_1}{4\varepsilon}\right)\|\delta_{tt}\phi^{n+1}\|_\Omega^2-\left(\frac{B_2}{2}-\frac{L_2}{4\delta}\right)\|\delta_t\psi^{n+1}\|_\Gamma^2-\frac{\tau}{K}\|\mu_\Gamma^{n+\frac{1}{2}}-\mu^{n+\frac{1}{2}}\|_\Gamma^2, \end{aligned} \tag{3.9}$$

where

$$\tilde{E}(\phi^{n+1},\psi^{n+1})=E^{total}(\phi^{n+1},\psi^{n+1})+\left(\frac{L_1}{4\varepsilon}+\frac{B_1}{2}\right)\|\delta_t\phi^{n+1}\|_\Omega^2+\left(\frac{L_2}{4\delta}+\frac{B_2}{2}\right)\|\delta_t\psi_\Gamma^{n+1}\|_\Gamma^2. \tag{3.10}$$

Proof. Pairing (3.1) with $\tau\mu^{n+\frac{1}{2}}$, we obtain

$$\left(\frac{\phi^{n+1}-\phi^n}{\tau},\tau\mu^{n+\frac{1}{2}}\right)_\Omega=\tau(\Delta\mu^{n+\frac{1}{2}},\mu^{n+\frac{1}{2}})_\Omega=\tau(\partial_{\mathbf{n}}\mu^{n+\frac{1}{2}},\mu^{n+\frac{1}{2}})_\Gamma-\tau(\nabla\mu^{n+\frac{1}{2}},\nabla\mu^{n+\frac{1}{2}})_\Omega.$$

Pairing (3.2) with $-\delta_t\phi^{n+1}$, we obtain

$$\begin{aligned}
&(-\delta_t\phi^{n+1},\mu^{n+\frac{1}{2}})_\Omega\\
=&-\varepsilon\left(\nabla(\phi^{n+1}-\phi^n),\nabla\left(\frac{\phi^{n+1}+\phi^n}{2}\right)\right)_\Omega+\varepsilon\left(\delta_t\phi^{n+1},\partial_{\mathbf{n}}\left(\frac{\phi^{n+1}+\phi^n}{2}\right)\right)_\Gamma\\
&-\frac{1}{\varepsilon}\left(\delta_t\phi^{n+1},f\left(\frac{3}{2}\phi^n-\frac{1}{2}\phi^n\right)\right)_\Omega+\left(\delta_t\phi^{n+1},A\tau\Delta(\phi^{n+1}-\phi^n)\right)_\Omega\\
&-B_1(\delta_t\phi^{n+1},\phi^{n+1}-2\phi^n+\phi^{n-1})_\Omega.
\end{aligned}\tag{3.11}$$

Pairing (3.1) with $2\sqrt{A}\tau\delta_t\phi^{n+1}$, we obtain

$$\begin{aligned}
&2\sqrt{A}\tau\|\delta_t\phi^{n+1}\|^2_\Omega=2\sqrt{A}\tau(\Delta\mu^{n+\frac{1}{2}},\delta_t\phi^{n+1})_\Omega\\
=&2\sqrt{A}\tau(\partial_{\mathbf{n}}\mu^{n+\frac{1}{2}},\delta_t\phi^{n+1})_\Gamma-2\sqrt{A}\tau(\nabla\mu^{n+\frac{1}{2}},\nabla\delta_t\phi^{n+1})_\Omega\\
\leq&2\sqrt{A}\tau(\partial_{\mathbf{n}}\mu^{n+\frac{1}{2}},\delta_t\phi^{n+1})_\Gamma+\tau\|\nabla\mu^{n+\frac{1}{2}}\|^2_\Omega+A\tau\|\nabla\delta_t\phi^{n+1}\|^2_\Omega.
\end{aligned}$$

Expanding $F(\phi^{n+1})$ and $F(\phi^n)$ at $\hat{\phi}^{n+\frac{1}{2}}$ yields

$$F(\phi^{n+1})=F(\hat{\phi}^{n+\frac{1}{2}})+f(\hat{\phi}^{n+\frac{1}{2}})(\phi^{n+1}-\hat{\phi}^{n+\frac{1}{2}})+\frac{1}{2}f'(\xi_1^n)(\phi^{n+1}-\hat{\phi}^{n+\frac{1}{2}})^2,$$

and

$$F(\phi^n)=F(\hat{\phi}^{n+\frac{1}{2}})+f(\hat{\phi}^{n+\frac{1}{2}})(\phi^n-\hat{\phi}^{n+\frac{1}{2}})+\frac{1}{2}f'(\xi_2^n)(\phi^n-\hat{\phi}^{n+\frac{1}{2}})^2,$$

where ξ_1^n is between ϕ^{n+1} and $\hat{\phi}^{n+\frac{1}{2}}$, ξ_2^n is between ϕ^n and $\hat{\phi}^{n+\frac{1}{2}}$. Subtracting the above two equations, we obtain

$$\begin{aligned}
&F(\phi^{n+1})-F(\phi^n)-f(\hat{\phi}^{n+\frac{1}{2}})\delta_t\phi^{n+1}\\
=&\frac{1}{2}f'(\xi_1^n)\delta_t\phi^{n+1}\delta_{tt}\phi^{n+1}-\frac{1}{8}(f'(\xi_2^n)-f'(\xi_1^n))(delta_t\phi^n)^2\\
\leq&\frac{L_1}{4}(|\delta_t\phi^{n+1}|^2+|\delta_{tt}\phi^{n+1}|^2)+\frac{L_1}{4}|\delta_t\phi^n|^2.
\end{aligned}$$

Multiplying the above equation with $\frac{1}{\varepsilon}$, then taking integration leads to

$$\frac{1}{\varepsilon}\left(F(\phi^{n+1})-F(\phi^n)-f(\phi^{n+\frac{1}{2}})\delta_t\phi^{n+1},1\right)_\Omega\leq\frac{L_1}{4\varepsilon}(\|\delta_t\phi^{n+1}\|^2_\Omega+\|\delta_{tt}\phi^{n+1}\|^2_\Omega+\|\delta_t\phi^n\|^2_\Omega).$$

For the term involving B_1 in equation (3.11),

$$-B_1(\delta_t\phi^{n+1},\phi^{n+1}-2\phi^n+\phi^{n-1})_\Omega=-\frac{B_1}{2}\|\delta_t\phi^{n+1}\|^2_\Omega+\frac{B_1}{2}\|\delta_t\phi^n\|^2_\Omega-\frac{B_1}{2}\|\delta_{tt}\phi^{n+1}\|^2_\Omega.$$

Summing up the above equations, we obtain

$$\begin{aligned}
&\frac{\varepsilon}{2}(\|\nabla\phi^{n+1}\|^2_\Omega-\|\nabla\phi^n\|^2_\Omega)+\frac{1}{\varepsilon}\left(F(\phi^{n+1})-F(\phi^n),1\right)_\Omega\\
&\quad-\varepsilon\left(\delta_t\phi^{n+1},\partial_{\mathbf{n}}\left(\frac{\phi^{n+1}+\phi^n}{2}\right)\right)_\Gamma+\frac{B_1}{2}\|\delta_t\phi^{n+1}\|^2-\frac{B_1}{2}\|\delta_t\phi^n\|^2\\
&\le-2\sqrt{A}\|\delta_t\phi^{n+1}\|^2_\Omega+2\sqrt{A}\tau(\partial_{\mathbf{n}}\mu^{n+\frac{1}{2}},\delta_t\phi^{n+1})_\Gamma+\tau(\partial_{\mathbf{n}}\mu^{n+\frac{1}{2}},\mu^{n+\frac{1}{2}})_\Gamma+A\tau(\partial_{\mathbf{n}}\delta_t\phi^{n+1},\delta_t\phi^{n+1})_\Gamma\\
&\quad+\frac{L_1}{4\varepsilon}\|\delta_t\phi^{n+1}\|^2_\Omega+\frac{L_1}{4\varepsilon}\|\delta_t\phi^n\|^2_\Omega-\frac{B_1}{2}\|\delta_{tt}\phi^n\|^2_\Omega+\frac{L_1}{4\varepsilon}\|\delta_{tt}\phi^n\|^2_\Omega. \qquad (3.12)
\end{aligned}$$

Similarly, pairing (3.5) with $\tau\mu_\Gamma^{n+\frac{1}{2}}$, we obtain

$$\left(\frac{\psi^{n+1}-\psi^n}{\tau},\tau\mu_\Gamma^{n+\frac{1}{2}}\right)_\Gamma=-\tau\|\nabla_\Gamma\mu_\Gamma^{n+\frac{1}{2}}\|^2_\Gamma-\tau(\partial_{\mathbf{n}}\mu^{n+\frac{1}{2}},\mu_\Gamma^{n+\frac{1}{2}})_\Gamma.$$

Pairing (3.6) with $-\delta_t\psi^{n+1}$, we obtain

$$\begin{aligned}
&(-\delta_t\psi^{n+1},\mu_\Gamma^{n+\frac{1}{2}})_\Gamma\\
=&-\delta\kappa\left(\nabla_\Gamma(\psi^{n+1}-\psi^n),\nabla_\Gamma\left(\frac{\psi^{n+1}+\psi^n}{2}\right)\right)-\frac{1}{\delta}\left(\delta_t\psi^{n+1},g\left(\frac{3}{2}\psi^n-\frac{1}{2}\psi^n\right)\right)_\Gamma\\
&-\varepsilon\left(\delta_t\psi^{n+1},\partial_n\left(\frac{\phi^{n+1}+\phi^n}{2}\right)\right)_\Gamma-A\tau\|\nabla_\Gamma\delta_t\psi^{n+1}\|^2_\Gamma\\
&-B_2(\delta_t\psi^{n+1},\psi^{n+1}-2\psi^n+\psi^{n-1})_\Gamma-A\tau(\partial_{\mathbf{n}}(\phi^{n+1}-\phi^n),\delta_t\psi^{n+1})_\Gamma. \qquad (3.13)
\end{aligned}$$

Pairing (3.5) with $2\sqrt{A}\tau\delta_t\psi^{n+1}$, we obtain

$$\begin{aligned}
2\sqrt{A}\|\delta_t\psi^{n+1}\|^2_\Gamma&=2\sqrt{A}\tau(\Delta_\Gamma\mu_\Gamma^{n+\frac{1}{2}}-\partial_{\mathbf{n}}\mu^{n+\frac{1}{2}},\delta_t\psi^{n+1})_\Gamma\\
&\le-2\sqrt{A}\tau(\partial_{\mathbf{n}}\mu^{n+\frac{1}{2}},\delta_t\psi^{n+1})_\Gamma+\tau\|\nabla_\Gamma\mu^{n+\frac{1}{2}}\|^2_\Gamma+A\tau\|\nabla_\Gamma\delta_t\psi^{n+1}\|^2_\Gamma.
\end{aligned}$$

The treatment of the term involving g is the same as that of the term involving f. Expanding $G(\psi^{n+1})$ and $G(\psi^n)$ at $\hat{\psi}^{n+\frac{1}{2}}$ and subtracting each other yields

$$G(\psi^{n+1})-G(\psi^n)-g(\hat{\psi}^{n+1})\delta_t\psi^{n+\frac{1}{2}}\le\frac{L_2}{4}(|\delta_t\psi^{n+1}|^2+|\delta_{tt}\psi^{n+1}|^2)+\frac{L_2}{4}|\delta_t\psi^n|^2,$$

Multiplying the above equation with $\frac{1}{\delta}$, then taking integration leads to

$$\frac{1}{\delta}(G(\psi^{n+1})-G(\psi^n)-g(\psi^{n+\frac{1}{2}})\delta_t\psi^{n+1},1)_\Gamma\le\frac{L_2}{4\delta}(\|\delta_t\psi^{n+1}\|^2_\Gamma+\|\delta_{tt}\psi^{n+1}\|^2_\Gamma+\|\delta_t\psi^n\|^2_\Gamma).$$

For the term involving B_2 in (3.13),

$$-B_2(\delta_t\psi^{n+1},\psi^{n+1}-2\psi^n+\psi^{n-1})_\Gamma=-\frac{B_2}{2}\|\delta_t\psi^{n+1}\|^2_\Gamma+\frac{B_2}{2}\|\delta_t\psi^n\|^2_\Gamma-\frac{B_2}{2}\|\delta_{tt}\psi^{n+1}\|^2_\Gamma.$$

Summing up the above equations, we obtain

$$\begin{aligned}
&\frac{\delta\kappa}{2}(\|\nabla_\Gamma\psi^{n+1}\|_\Omega^2-\|\nabla_\Gamma\psi^n\|_\Gamma^2)+\frac{1}{\delta}\Big(G(\psi^{n+1})-G(\psi^n),1\Big)_\Gamma\\
&\quad+\varepsilon\left(\delta_t\psi^{n+1},\partial_{\mathbf{n}}\left(\frac{\phi^{n+1}+\phi^n}{2}\right)\right)_\Gamma+\frac{B_2}{2}\|\delta_t\psi^{n+1}\|^2-\frac{B_2}{2}\|\delta_t\psi^n\|^2\\
&\leq-2\sqrt{A}\|\delta_t\psi^{n+1}\|_\Gamma^2-2\sqrt{A}\tau(\partial_{\mathbf{n}}\mu^{n+\frac{1}{2}},\delta_t\psi^{n+1})_\Gamma-\tau(\partial_{\mathbf{n}}\mu^{n+\frac{1}{2}},\mu_\Gamma^{n+\frac{1}{2}})_\Gamma\\
&\quad-A\tau(\partial_{\mathbf{n}}\delta_t\phi^{n+1},\delta_t\psi^{n+1})_\Gamma+\frac{L_2}{4\delta}\|\delta_t\psi^{n+1}\|_\Gamma^2+\frac{L_2}{4\delta}\|\delta_t\psi^n\|_\Gamma^2\\
&\quad-\frac{B_2}{2}\|\delta_{tt}\psi^{n+1}\|_\Gamma^2+\frac{L_2}{4\delta}\|\delta_{tt}\psi^n\|_\Gamma^2.
\end{aligned}\tag{3.14}$$

Combining the results in (3.12) and (3.14), we have

$$\begin{aligned}
&\frac{\varepsilon}{2}(\|\nabla\phi^{n+1}\|_\Omega^2-\|\nabla\phi^n\|_\Omega^2)+\frac{1}{\varepsilon}\Big(F(\phi^{n+1})-F(\phi^n),1\Big)_\Omega+\frac{B_1}{2}\|\delta_t\phi^{n+1}\|_\Omega^2-\frac{B_1}{2}\|\delta_t\phi^n\|_\Omega^2\\
&\quad+\frac{\delta\kappa}{2}(\|\nabla_\Gamma\psi^{n+1}\|_\Omega^2-\|\nabla_\Gamma\psi^n\|_\Gamma^2)+\frac{1}{\delta}\Big(G(\psi^{n+1})-G(\psi^n),1\Big)_\Gamma\\
&\quad+\frac{B_2}{2}\|\delta_t\psi^{n+1}\|_\Gamma^2-\frac{B_2}{2}\|\delta_t\psi^n\|_\Gamma^2\\
&\leq\Big(\frac{L_1}{4\varepsilon}-2\sqrt{A}\Big)\|\delta_t\phi^{n+1}\|_\Omega^2+\Big(\frac{L_2}{4\delta}-2\sqrt{A}\Big)\|\delta_t\psi^{n+1}\|_\Gamma^2-\frac{\tau}{K}\|\mu_\Gamma^{n+\frac{1}{2}}-\mu^{n+\frac{1}{2}}\|_\Gamma^2\\
&\quad+\Big(\frac{L_1}{4\varepsilon}-\frac{B_1}{2}\Big)\|\delta_{tt}\phi^{n+1}\|_\Omega^2+\Big(\frac{L_2}{4\delta}-\frac{B_2}{2}\Big)\|\delta_{tt}\psi^{n+1}\|_\Gamma^2+\frac{L_1}{4\varepsilon}\|\delta_t\phi^n\|_\Omega^2+\frac{L_2}{4\delta}\|\delta_t\psi^n\|_\Gamma^2.
\end{aligned}$$

Then under the conditions (3.7)-(3.8), for the modified energy (3.22), the estimate (3.9) holds. □

Remark 3.1. The GMS model and Liu-Wu model are the same as KLLM model, except for the boundary conditions. And thus, similarly, the second-order scheme for the boundary equations of the GMS model (1.6) reads as follows,

$$\begin{cases}
\phi^{n+1}|_\Gamma=\psi^{n+1}, & \mathbf{x}\in\Gamma, \quad (3.15)\\
\dfrac{\psi^{n+1}-\psi^n}{\tau}=\Delta_\Gamma\mu^{n+\frac{1}{2}}-\partial_{\mathbf{n}}\mu^{n+\frac{1}{2}}, & \mathbf{x}\in\Gamma, \quad (3.16)\\
\mu^{n+\frac{1}{2}}=-\delta\kappa\Delta_\Gamma\left(\dfrac{\psi^{n+1}+\psi^n}{2}\right)+\dfrac{1}{\delta}g\left(\dfrac{3}{2}\psi^n-\dfrac{1}{2}\psi^{n-1}\right)+\varepsilon\partial_{\mathbf{n}}\left(\dfrac{\phi^{n+1}+\phi^n}{2}\right) & \\
\qquad -A\tau\Delta_\Gamma\left(\psi^{n+1}-\psi^n\right)+B_2\left(\psi^{n+1}-2\psi^n+\psi^{n-1}\right)+A\tau\partial_{\mathbf{n}}\left(\phi^{n+1}-\phi^n\right), & \mathbf{x}\in\Gamma. \quad (3.17)
\end{cases}$$

And the second-order scheme for the boundary equations of Liu-Wu model (1.7) reads,

$$
\begin{cases}
\phi^{n+1}|_\Gamma = \psi^{n+1}, & \mathbf{x}\in\Gamma, \quad (3.18)\\
\partial_{\mathbf{n}}\mu^{n+\frac{1}{2}} = 0, & \mathbf{x}\in\Gamma, \quad (3.19)\\
\dfrac{\psi^{n+1}-\psi^n}{\tau} = \Delta_\Gamma \mu_\Gamma^{n+\frac{1}{2}}, & \mathbf{x}\in\Gamma, \quad (3.20)\\
\mu_\Gamma^{n+\frac{1}{2}} = -\delta\kappa\Delta_\Gamma\left(\dfrac{\psi^{n+1}+\psi^n}{2}\right) + \dfrac{1}{\delta}g\left(\dfrac{3}{2}\psi^n - \dfrac{1}{2}\psi^{n-1}\right) + \varepsilon\partial_{\mathbf{n}}\left(\dfrac{\phi^{n+1}+\phi^n}{2}\right) & \\
\qquad -A\tau\Delta_\Gamma\left(\psi^{n+1}-\psi^n\right) + B_2\left(\psi^{n+1}-2\psi^n+\psi^{n-1}\right) + A\tau\partial_{\mathbf{n}}\left(\phi^{n+1}-\phi^n\right), & \mathbf{x}\in\Gamma. \quad (3.21)
\end{cases}
$$

The energy stability of the above two schemes are similar to (3.1), where

$$
\tilde{E}(\phi^{n+1},\psi^{n+1}) = E^{total}(\phi^{n+1},\psi^{n+1}) + \left(\frac{L_1}{4\varepsilon}+\frac{B_1}{2}\right)\|\delta_t\phi^{n+1}\|_\Omega^2 + \left(\frac{L_2}{4\delta}+\frac{B_2}{2}\right)\|\delta_t\psi_\Gamma^{n+1}\|_\Gamma^2. \tag{3.22}
$$

Compared with $\tilde{E}(\phi^{n+1},\psi^{n+1})$ in (3.9), the item related to K and the difference between chemical potential is missing. And the proof of energy stability of GMS model and Liu-Wu model are also similar to the case of KLLM model (see Theorem 3.1).

Remark 3.2. If $B_1 = B_2 = 0$, we can take

$$
A \geq \max\left\{\frac{9L_1^2}{16\varepsilon^2}, \frac{9L_2^2}{16\delta^2}\right\}
$$

to make the SL-CN scheme unconditionally stable as well. The numerical results show that A can take much smaller values in practice than theoretical one when nonzero B values are used.

Remark 3.3. It should be noted that term $\partial_{\mathbf{n}}\mu^{n+\frac{1}{2}}$ derived by integration by parts makes a major difference among the three kinds of boundary conditions. In KLLM model, $(\partial_{\mathbf{n}}\mu^{n+\frac{1}{2}},\mu^{n+\frac{1}{2}})_\Gamma$ and $(\partial_{\mathbf{n}}\mu^{n+\frac{1}{2}},\mu_\Gamma^{n+\frac{1}{2}})_\Gamma$ can be combined into $K\|\mu_\Gamma^{n+\frac{1}{2}}-\mu^{n+\frac{1}{2}}\|_\Gamma^2$ by condition (3.3), while these two terms can offset each other in GMS model and $\partial_{\mathbf{n}}\mu^{n+\frac{1}{2}} = 0$ in Liu-Wu model. Due to the above illustrations, we have similar stability theorems for different boundary conditions.

4 Convergence analysis

We will establish the error estimate of the semi-discretized SL-CN scheme (3.1)-(3.6) of the KLLM model (1.5) in detail. For the convergence of scheme (3.15)-(3.17) of GMS model (1.6) and scheme (3.18)-(3.21) of Liu-Wu model (1.7) see Remark 4.1. Here, the mathematical induction is utilized and the trace theorem is applied to estimate the boundary terms.

Let $\phi(t^n)$, $\psi(t^n)$ be the exact solution at time $t=t^n$ to equation (1.5) and ϕ^n, ψ^n be the solution at time $t=t^n$ to the numerical scheme (3.1)-(3.6). Define the error functions

$$e_\phi^n=\phi^n-\phi(t^n),\quad e_\psi^n=\psi^n-\psi(t^n),\quad e_\mu^n=\mu^n-\mu(t^n),\quad e_\Gamma^n=\mu_\Gamma^n-\mu_\Gamma(t^n).$$

We assume that the exact solution $(\phi,\psi,\mu,\mu_\Gamma)$ of the system (1.5) is sufficiently smooth, or possesses the following regularity

$$\begin{aligned}&\phi,\phi_t,\phi_{tt}\in L^\infty(0,T;H^{m_1}(\Omega));\\&\mu\in L^\infty(0,T;H^{m_2}(\Omega));\\&\mu_\Gamma\in L^\infty(0,T;H^{m_3}(\Omega));\end{aligned}$$

with m_1,m_2,m_3 sufficiently large (the assumption that $m_1\geq\frac{7}{2}$, $m_2\geq\frac{3}{2}$, $m_3\geq 1$ is suitable for the following error analysis). Due to the trace theorem and the linearity of the trace operator, the trace ψ possesses the regularity

$$\psi,\psi_t,\psi_{tt}\in L^\infty(0,T;H^{m_1-\frac{1}{2}}(\Gamma)).$$

A careful consistency analysis implies that

$$\begin{cases}\dfrac{\phi(t^{n+1})-\phi(t^n)}{\tau}=\Delta\mu(t^{n+\frac12})+R_\phi^{n+1}, & \mathbf{x}\in\Omega, \quad (4.1)\\ \mu^{n+\frac12}=-\varepsilon\Delta\left(\dfrac{\phi(t^{n+1})+\phi(t^n)}{2}\right)+\dfrac{1}{\varepsilon}f\left(\dfrac32\phi(t^n)-\dfrac12\phi(t^{n-1})\right) & \\ \qquad -A\tau\Delta\Big(\phi(t^{n+1})-\phi(t^n)\Big)+B_1\Big(\phi(t^{n+1})-2\phi(t^n)+\phi(t^{n-1})\Big)+R_\mu^{n+\frac12}, & \mathbf{x}\in\Omega, \quad (4.2)\\ K\partial_{\mathbf{n}}\mu(t^{n+\frac12})=\mu_\Gamma(t^{n+\frac12})-\mu(t^{n+\frac12}), & \mathbf{x}\in\Gamma, \quad (4.3)\\ \phi(t^{n+1})|_\Gamma=\psi(t^{n+1}), & \mathbf{x}\in\Gamma, \quad (4.4)\\ \dfrac{\psi(t^{n+1})-\psi(t^n)}{\tau}=\Delta_\Gamma\mu_\Gamma(t^{n+\frac12})-\partial_{\mathbf{n}}\mu(t^{n+\frac12})+R_\psi^{n+1}, & \mathbf{x}\in\Gamma, \quad (4.5)\\ \mu_\Gamma(t^{n+1})=-\delta\kappa\Delta_\Gamma\left(\dfrac{\psi(t^{n+1})+\psi(t^n)}{2}\right)+\dfrac{1}{\delta}g\left(\dfrac32\psi(t^n)-\dfrac12\psi(t^{n-1})\right) & \\ \qquad +\varepsilon\partial_{\mathbf{n}}\left(\dfrac{\phi(t^{n+1})+\phi(t^n)}{2}\right) & \\ \qquad -A\tau\Delta_\Gamma\Big(\psi(t^{n+1})-\psi(t^n)\Big)+B_2\Big(\psi(t^{n+1})-2\psi(t^n)+\psi(t^{n-1})\Big) & \\ \qquad +A\tau\partial_{\mathbf{n}}\Big(\phi(t^{n+1})-\phi(t^n)\Big)+R_\Gamma^{n+\frac12}, & \mathbf{x}\in\Gamma, \quad (4.6)\end{cases}$$

where the residual terms are

$$
\begin{aligned}
R_\phi^{n+\frac{1}{2}} &= \frac{\phi(t^{n+1})-\phi(t^n)}{\tau} - \phi_t(t^{n+\frac{1}{2}}),\\
R_\psi^{n+\frac{1}{2}} &= \frac{\psi(t^{n+1})-\psi(t^n)}{\tau} - \psi_t(t^{n+\frac{1}{2}}),\\
R_\mu^{n+\frac{1}{2}} &= \varepsilon\Delta\left(\frac{\phi(t^{n+1})+\phi(t^n)}{2}\right) - \varepsilon\Delta\phi(t^{n+\frac{1}{2}}) + \frac{1}{\varepsilon}f\left(\phi(t^{n+\frac{1}{2}})\right) - \frac{1}{\varepsilon}f\left(\frac{3}{2}\phi(t^n)-\frac{1}{2}\phi(t^{n-1})\right)\\
&\quad + A\tau\Delta\left(\phi(t^{n+1})-\phi(t^n)\right) - B_1\left(\phi(t^{n+1})-2\phi(t^n)+\phi(t^{n-1})\right),\\
R_\Gamma^{n+\frac{1}{2}} &= \delta\kappa\Delta_\Gamma\left(\frac{\psi(t^{n+1})+\psi(t^n)}{2}\right) - \delta\kappa\Delta_\Gamma\psi(t^{n+\frac{1}{2}})\\
&\quad + \frac{1}{\delta}g\left(\psi(t^{n+\frac{1}{2}})\right) - \frac{1}{\delta}g\left(\frac{3}{2}\psi(t^n)-\frac{1}{2}\psi(t^{n-1})\right)\\
&\quad + \varepsilon\partial_{\mathbf{n}}\phi(t^{n+\frac{1}{2}}) - \varepsilon\partial_{\mathbf{n}}\left(\frac{\phi(t^{n+1})+\phi(t^n)}{2}\right) + A\tau\Delta\left(\psi(t^{n+1})-\psi(t^n)\right)\\
&\quad - B_2\left(\psi(t^{n+1})-2\psi(t^n)+\psi(t^{n-1})\right) - A\tau\partial_{\mathbf{n}}\left(\phi(t^{n+1})-\phi(t^n)\right).
\end{aligned}
$$

Using the Taylor expansion and regularity of ϕ and ψ, it's easy to prove the following Lemma 4.1.

Lemma 4.1. *The truncation errors satisfy*

$$
\begin{aligned}
&\|R_{\phi,\tau}\|_{l^\infty(H^1(\Omega))} + \|R_{\mu,\tau}\|_{l^\infty(H^1(\Omega))} \lesssim \tau^2,\\
&\|R_{\psi,\tau}\|_{l^\infty(H^1(\Gamma))} + \|R_{\Gamma,\tau}\|_{l^\infty(H^1(\Gamma))} \lesssim \tau^2.
\end{aligned}
$$

Thus we can establish the estimates for the scheme (3.1)-(3.6) as follows.

Theorem 4.1. *Suppose that the exact solutions $(\phi,\psi,\mu,\mu_\Gamma)$ are sufficiently smooth and Assumption 1 holds. Then $\forall\tau\le\tau_0$, we have the following error estimate for the SL-CN scheme* (3.1)-(3.6),

$$
\|e_{\phi,\tau}\|_{l^\infty(H^1(\Omega))} + \|e_{\psi,\tau}\|_{l^\infty(H^1(\Gamma))} \lesssim \tau^2.
$$

Proof. By subtracting (3.1)-(3.6) from the corresponding scheme (4.1)-(4.6) we derive the error equations as follows,

$$\begin{cases} \dfrac{e_\phi^{n+1}-e_\phi^n}{\tau}=\Delta e_\mu^{n+\frac{1}{2}}+R_\phi^{n+\frac{1}{2}}, & \mathbf{x}\in\Omega, \quad (4.7)\\ e_\mu^{n+\frac{1}{2}}=-\varepsilon\Delta\left(\dfrac{e_\phi^{n+1}+e_\phi^n}{2}\right)+\dfrac{1}{\varepsilon}\left(f\left(\dfrac{3}{2}\phi(t^n)-\dfrac{1}{2}\phi(t^{n-1})\right)-f\left(\dfrac{3}{2}\phi^n-\dfrac{1}{2}\phi^{n-1}\right)\right) & \\ \qquad -A\tau\Delta(e_\phi^{n+1}-e_\phi^n)+B_1(e_\phi^{n+1}-2e_\phi^n+e_\phi^{n-1})+R_\mu^{n+\frac{1}{2}}, & \mathbf{x}\in\Omega, \quad (4.8)\\ K\partial_{\mathbf{n}}e_\mu^{n+\frac{1}{2}}=e_\Gamma^{n+\frac{1}{2}}-e_\mu^{n+\frac{1}{2}}, & \mathbf{x}\in\Gamma, \quad (4.9)\\ e_\phi^{n+1}|_\Gamma=e_\psi^{n+1}, & \mathbf{x}\in\Gamma, \quad (4.10)\\ \dfrac{e_\psi^{n+1}-e_\psi^n}{\tau}=\Delta_\Gamma e_\Gamma^{n+\frac{1}{2}}-\partial_{\mathbf{n}}e_\mu^{n+\frac{1}{2}}+R_\psi^{n+\frac{1}{2}}, & \mathbf{x}\in\Gamma, \quad (4.11)\\ e_\Gamma^{n+\frac{1}{2}}=-\delta\kappa\Delta_\Gamma\left(\dfrac{e_\psi^{n+1}+e_\psi^n}{2}\right)+\dfrac{1}{\delta}\left(g\left(\dfrac{3}{2}\psi(t^{n+1})-\dfrac{1}{2}\psi(t^n)\right)\right. & \\ \qquad \left.-g\left(\dfrac{3}{2}\psi^n-\dfrac{1}{2}\psi^{n-1}\right)\right)+\varepsilon\partial_{\mathbf{n}}\left(\dfrac{e_\psi^{n+1}+e_\psi^n}{2}\right)-A\tau\Delta_\Gamma(e_\psi^{n+1}-e_\psi^n) & \\ \qquad +B_2(e_\psi^{n+1}-2e_\psi^n+e_\psi^{n-1})+A\tau\partial_{\mathbf{n}}(e_\phi^{n+1}-e_\phi^n)+R_\Gamma^{n+\frac{1}{2}}, & \mathbf{x}\in\Gamma. \quad (4.12) \end{cases}$$

We use the mathematical induction to prove this theorem. When $m=0$, we have $e_\phi^0=e_\psi^0=\nabla e_\phi^0=\nabla_\Gamma e_\psi^0=0$. Obviously, Theorem 4.1 holds. Assuming that Theorem 4.1 holds for all $n\leq m$, we need to show that Theorem 4.1 holds for e_ϕ^{m+1} and e_ψ^{m+1}.

For each $n\leq m$, pairing (4.7) with $\tau e_\mu^{n+\frac{1}{2}}$, we have

$$(e_\phi^{n+1}-e_\phi^n,e_\mu^{n+\frac{1}{2}})_\Omega+\tau\|\nabla e_\mu^{n+\frac{1}{2}}\|_\Omega^2=\tau(\partial_{\mathbf{n}}e_\mu^{n+\frac{1}{2}},e_\mu^{n+\frac{1}{2}})_\Gamma+\tau(R_\phi^{n+\frac{1}{2}},e_\mu^{n+\frac{1}{2}})_\Omega.$$

Pairing (4.7) with $\varepsilon\tau e_\phi^{n+1}$,

$$\begin{aligned} &\frac{\varepsilon}{2}(\|e_\phi^{n+1}\|_\Omega^2-\|e_\phi^n\|_\Omega^2+\|e_\phi^{n+1}-e_\phi^{n+1}\|_\Omega^2)\\ =&-\varepsilon\tau(\nabla e_\mu^{n+\frac{1}{2}},\nabla e_\phi^{n+1})_\Omega+\varepsilon\tau(\partial_{\mathbf{n}}e_\mu^{n+\frac{1}{2}},e_\phi^{n+1})_\Gamma+\varepsilon\tau(R_\phi^{n+\frac{1}{2}},e_\phi^{n+1})_\Omega. \end{aligned}$$

By taking the L^2 inner product of (4.8) with $-(e_\phi^{n+1}-e_\phi^{n+1})$ in Ω, we have

$$\begin{aligned} -(e_\mu^{n+\frac{1}{2}},e_\phi^{n+1}-e_\phi^n)_\Omega=&-\frac{\varepsilon}{2}(\|\nabla e_\phi^{n+1}\|_\Omega^2-\|\nabla e_\phi^n\|_\Omega^2)+\varepsilon\left(\partial_{\mathbf{n}}\left(\frac{e_\phi^{n+1}+e_\phi^n}{2}\right),e_\phi^{n+1}-e_\phi^n\right)_\Gamma\\ &-\frac{1}{\varepsilon}\left(f\left(\frac{3}{2}\phi(t^n)-\frac{1}{2}\phi(t^{n-1})\right)-f\left(\frac{3}{2}\phi^n-\frac{1}{2}\phi^{n-1}\right),e_\phi^{n+1}-e_\phi^n\right)_\Omega \end{aligned}$$

$$
\begin{aligned}
&+A\tau(\partial_{\mathbf{n}}(e_\phi^{n+1}-e_\phi^n),e_\phi^{n+1}-e_\phi^n)_\Gamma - A\tau(\nabla(e_\phi^{n+1}-e_\phi^n),\nabla(e_\phi^{n+1}-e_\phi^n))_\Omega \\
&-B_1(e_\phi^{n+1}-2e_\phi^n+e_\phi^{n-1},e_\phi^{n+1}-e_\phi^n)_\Omega-(R_\mu^{n+\frac{1}{2}},e_\phi^{n+1}-e_\phi^n)_\Omega.
\end{aligned}
$$

Combining the equations above, we derive

$$
\begin{aligned}
&\frac{\varepsilon}{2}(\|\nabla e_\phi^{n+1}\|_\Omega^2-\|\nabla e_\phi^n\|_\Omega^2)+\frac{\varepsilon}{2}(\|e_\phi^{n+1}\|_\Omega^2-\|e_\phi^n\|_\Omega^2+\|e_\phi^{n+1}-e_\phi^{n+1}\|_\Omega^2) \\
&+A\tau\|\nabla(e_\phi^{n+1}-e_\phi^n)\|_\Omega^2+\tau\|\nabla e_\mu^{n+\frac{1}{2}}\|_\Omega^2 \\
&+\frac{B_1}{2}(\|e_\phi^{n+1}-e_\phi^n\|_\Omega^2-\|e_\phi^n-e_\phi^{n-1}\|_\Omega^2+\|e_\phi^{n+1}-2e_\phi^n-e_\phi^{n-1}\|_\Omega^2) \\
=&\tau(\partial_{\mathbf{n}}e_\mu^{n+\frac{1}{2}},e_\mu^{n+\frac{1}{2}})_\Gamma+\tau(R_\phi^{n+\frac{1}{2}},e_\mu^{n+\frac{1}{2}})_\Omega-\varepsilon\tau(\nabla e_\mu^{n+\frac{1}{2}},\nabla e_\phi^{n+1})_\Omega \\
&+\varepsilon\tau(\partial_{\mathbf{n}}e_\mu^{n+\frac{1}{2}},e_\phi^{n+1})_\Gamma+\varepsilon\tau(R_\phi^{n+\frac{1}{2}},e_\phi^{n+1})_\Omega+\varepsilon\left(\partial_{\mathbf{n}}\left(\frac{e_\phi^{n+1}+e_\phi^n}{2}\right),e_\phi^{n+1}-e_\phi^n\right)_\Gamma \\
&-\frac{1}{\varepsilon}\left(f\left(\frac{3}{2}\phi(t^n)-\frac{1}{2}\phi(t^{n-1})\right)-f\left(\frac{3}{2}\phi^n-\frac{1}{2}\phi^{n-1}\right),e_\phi^{n+1}-e_\phi^n\right)_\Omega \\
&-(R_\mu^{n+\frac{1}{2}},e_\phi^{n+1}-e_\phi^n)_\Omega+A\tau(\partial_{\mathbf{n}}(e_\phi^{n+1}-e_\phi^n),e_\phi^{n+1}-e_\phi^n)_\Gamma. \qquad (4.13)
\end{aligned}
$$

For the boundary term, taking the L^2 inner product of (4.11) with $\tau e_\Gamma^{n+\frac{1}{2}}$, together with the L^2 inner product of (4.11) with $\varepsilon\tau e_\psi^{n+1}$ and adding the L^2 inner product of (4.12) with $-(e_\psi^{n+1}-e_\psi^n)$ on Γ, we have

$$
\begin{aligned}
&\frac{\delta\kappa}{2}(\|\nabla_\Gamma e_\psi^{n+1}\|_\Gamma^2-\|\nabla e_\psi^n\|_\Gamma^2)+\frac{\varepsilon}{2}(\|e_\psi^{n+1}\|_\Gamma^2-\|e_\psi^n\|_\Gamma^2+\|e_\psi^{n+1}-e_\psi^{n+1}\|_\Gamma^2) \\
&+A\tau\|\nabla_\Gamma(e_\psi^{n+1}-e_\psi^n)\|_\Gamma^2+\tau\|\nabla_\Gamma e_\Gamma^{n+\frac{1}{2}}\|_\Gamma^2+\tau(\partial_{\mathbf{n}}e_\mu^{n+\frac{1}{2}},e_\Gamma^{n+\frac{1}{2}})_\Gamma \\
&+\frac{B_2}{2}(\|e_\psi^{n+1}-e_\psi^n\|_\Gamma^2-\|e_\psi^n-e_\psi^{n-1}\|_\Gamma^2+\|e_\psi^{n+1}-2e_\psi^n-e_\psi^{n-1}\|_\Gamma^2) \\
=&\tau(R_\psi^{n+\frac{1}{2}},e_\Gamma^{n+\frac{1}{2}})_\Gamma-\varepsilon\tau(\nabla_\Gamma e_\Gamma^{n+\frac{1}{2}},\nabla_\Gamma e_\psi^{n+1})_\Gamma \\
&-\varepsilon\tau(\partial_{\mathbf{n}}e_\mu^{n+\frac{1}{2}},e_\psi^{n+1})_\Gamma+\varepsilon\tau(R_\psi^{n+\frac{1}{2}},e_\psi^{n+1})_\Gamma-\varepsilon\left(\partial_{\mathbf{n}}\left(\frac{e_\phi^{n+1}+e_\phi^n}{2}\right),e_\psi^{n+1}-e_\psi^n\right)_\Gamma \\
&-\frac{1}{\delta}\left(g\left(\frac{3}{2}\psi(t^n)-\frac{1}{2}\psi(t^{n-1})\right)-g\left(\frac{3}{2}\psi^n-\frac{1}{2}\psi^{n-1}\right),e_\psi^{n+1}-e_\psi^n\right)_\Gamma \\
&-(R_\Gamma^{n+\frac{1}{2}},e_\psi^{n+1}-e_\psi^n)_\Gamma-A\tau(\partial_{\mathbf{n}}(e_\phi^{n+1}-e_\phi^n),e_\psi^{n+1}-e_\psi^n)_\Gamma. \qquad (4.14)
\end{aligned}
$$

By putting (4.13) and (4.14) together, we derive

$$\begin{aligned}
&\frac{\varepsilon}{2}(\|\nabla e_\phi^{n+1}\|_\Omega^2-\|\nabla e_\phi^n\|_\Omega^2)+\frac{\varepsilon}{2}(\|e_\phi^{n+1}\|_\Omega^2-\|e_\phi^n\|_\Omega^2+\|e_\phi^{n+1}-e_\phi^{n+1}\|_\Omega^2)\\
&\quad+A\tau(\|\nabla(e_\phi^{n+1}-e_\phi^n)\|_\Omega^2+\|\nabla_\Gamma(e_\psi^{n+1}-e_\psi^n)\|_\Gamma^2)\\
&\quad+\frac{B_1}{2}(\|e_\phi^{n+1}-e_\phi^n\|_\Omega^2-\|e_\phi^n-e_\phi^{n-1}\|_\Omega^2+\|e_\phi^{n+1}-2e_\phi^n-e_\phi^{n-1}\|_\Omega^2)\\
&\quad+\frac{\delta\kappa}{2}(\|\nabla_\Gamma e_\psi^{n+1}\|_\Gamma^2-\|\nabla e_\psi^n\|_\Gamma^2)+\frac{\varepsilon}{2}(\|e_\psi^{n+1}\|_\Gamma^2-\|e_\psi^n\|_\Gamma^2+\|e_\psi^{n+1}-e_\psi^{n+1}\|_\Gamma^2)\\
&\quad+\frac{B_2}{2}(\|e_\psi^{n+1}-e_\psi^n\|_\Gamma^2-\|e_\psi^n-e_\psi^{n-1}\|_\Gamma^2+\|e_\psi^{n+1}-2e_\psi^n-e_\psi^{n-1}\|_\Gamma^2)\\
&\quad+\tau\|\nabla e_\mu^{n+\frac12}\|_\Omega^2+\tau\|\nabla_\Gamma e_\Gamma^{n+\frac12}\|_\Gamma^2+K\tau\|\partial_{\mathbf{n}} e_\mu^{n+\frac12}\|_\Gamma^2\\
=&\varepsilon\tau(R_\phi^{n+\frac12},e_\phi^{n+1})_\Omega+\varepsilon\tau(R_\psi^{n+\frac12},e_\psi^{n+1})_\Gamma\quad(:=term\, M_1)\\
&\quad+\tau(R_\phi^{n+\frac12},e_\mu^{n+\frac12})_\Omega+\tau(R_\psi^{n+\frac12},e_\Gamma^{n+\frac12})_\Gamma\quad(:=term\, M_2)\\
&\quad-\varepsilon\tau(\nabla e_\mu^{n+\frac12},\nabla e_\phi^{n+1})_\Omega-\varepsilon\tau(\nabla_\Gamma e_\Gamma^{n+\frac12},\nabla_\Gamma e_\psi^{n+1})_\Gamma\quad(:=term\, M_3)\\
&\quad-\frac{1}{\varepsilon}\left(f\left(\frac32\phi(t^n)-\frac12\phi(t^{n-1})\right)-f\left(\frac32\phi^n-\frac12\phi^{n-1}\right),e_\phi^{n+1}-e_\phi^n\right)_\Omega\\
&\quad-(R_\mu^{n+\frac12},e_\phi^{n+1}-e_\phi^n)_\Omega\quad(:=term\, M_4)\\
&\quad-\frac{1}{\delta}\left(g\left(\frac32\psi(t^n)-\frac12\psi(t^{n-1})\right)-g\left(\frac32\psi^n-\frac12\psi^{n-1}\right),e_\psi^{n+1}-e_\psi^n\right)_\Gamma\\
&\quad-(R_\Gamma^{n+\frac12},e_\psi^{n+1}-e_\psi^n)_\Gamma\quad(:=term\, M_5).
\end{aligned}\tag{4.15}$$

The right hand side of (4.15) can be estimated term by term as below.

For M_1, we have

$$\begin{aligned}
&\varepsilon\tau(R_\phi^{n+\frac12},e_\phi^{n+1})_\Omega+\varepsilon\tau(R_\psi^{n+\frac12},e_\psi^{n+1})_\Gamma\\
\le&\varepsilon\tau\|R_\phi^{n+\frac12}\|_\Omega\|e_\phi^{n+1}\|_\Omega+\varepsilon\tau\|R_\psi^{n+\frac12}\|_\Gamma\|e_\psi^{n+1}\|_\Gamma\\
\le&\frac{\varepsilon\tau}{2}\|e_\phi^{n+1}\|_\Omega^2+\frac{\varepsilon\tau}{2}\|e_\psi^{n+1}\|_\Gamma^2+C_1\varepsilon\tau^5,
\end{aligned}\tag{4.16}$$

where C_1 is a constant independent of τ and ε. And the estimates for the truncation terms $R_\phi^{n+\frac12}$ and $R_\psi^{n+\frac12}$ are used in (4.16).

We define

$$H^{n,n-1}=f\left(\frac32\phi(t^n)-\frac12\phi(t^{n-1})\right)-f\left(\frac32\phi^n-\frac12\phi^{n-1}\right)$$

for simplicity. It can be rewritten as

$$\begin{aligned}H^{n,n-1}&=f(\hat{\phi}(t^n))-f(\hat{\phi}^n)\\&=(\hat{\phi}(t^n)-\hat{\phi}^n)\int_0^1 f'(s\hat{\phi}(t^n)+(1-s)\hat{\phi}^n)ds\\&=\left(\frac{3}{2}e_\phi^n-\frac{1}{2}e_\phi^{n-1}\right)\int_0^1 f'(s\hat{\phi}(t^n)+(1-s)\hat{\phi}^n)ds,\end{aligned}$$

where

$$\hat{\phi}(t^n)=\frac{3}{2}\phi(t^n)-\frac{1}{2}\phi(t^{n-1}),\quad \hat{\phi}^n=\frac{3}{2}\phi^n-\frac{1}{2}\phi^{n-1}.$$

Since f' is bounded, we have

$$\|H^{n,n-1}\|_\Omega\lesssim\|e_\phi^n\|_\Omega+\|e_\phi^{n-1}\|_\Omega.$$

By taking the gradient of $H^{n,n-1}$, we have

$$\begin{aligned}\nabla H^{n,n-1}&=f'(\hat{\phi}(t^n))\nabla\hat{\phi}(t^n)-f'(\hat{\phi}^n)\nabla\hat{\phi}^n\\&=\big(f'(\hat{\phi}(t^n))-f'(\hat{\phi}^n)\big)\nabla\hat{\phi}(t^n)+f'(\hat{\phi}^n)\nabla(\hat{\phi}(t^n)-\hat{\phi}^n).\end{aligned}$$

Since f' is bounded, Lipschitz continuous and $\phi\in L^\infty(0,T;H^{m_1})$, we have

$$\begin{aligned}\|\nabla H^{n,n-1}\|_\Omega&\lesssim\|\hat{\phi}(t^n)-\hat{\phi}^n\|_\Omega+\|\nabla(\hat{\phi}(t^n)-\hat{\phi}^n)\|_\Omega\\&\lesssim\|e_\phi^n\|_\Omega+\|e_\phi^{n-1}\|_\Omega+\|\nabla e_\phi^n\|_\Omega+\|\nabla e_\phi^{n-1}\|_\Omega.\end{aligned}$$

Similarly, we define

$$\tilde{H}^{n,n-1}=g\left(\frac{3}{2}\psi(t^n)-\frac{1}{2}\psi(t^{n-1})\right)-g\left(\frac{3}{2}\psi^n-\frac{1}{2}\psi^{n-1}\right).$$

Since g' is bounded, Lipschitz continuous and $\psi\in L^\infty(0,T;H^{m_1-\frac{1}{2}})$, we have

$$\|\tilde{H}^{n,n-1}\|_\Gamma\lesssim\|e_\psi^n\|_\Gamma+\|e_\psi^{n-1}\|_\Gamma,$$

and

$$\|\nabla_\Gamma\tilde{H}^{n,n-1}\|_\Gamma\lesssim\|e_\psi^n\|_\Gamma+\|e_\psi^{n-1}\|_\Gamma+\|\nabla_\Gamma e_\psi^n\|_\Gamma+\|\nabla_\Gamma e_\psi^{n-1}\|_\Gamma.$$

For the first term of M_2 in (4.15), we have

$$\begin{aligned}
&\tau(R_\phi^{n+\frac{1}{2}},e_\mu^{n+\frac{1}{2}})_\Omega\\
\leq&\frac{\varepsilon\tau}{2}\|\nabla R_\phi^{n+\frac{1}{2}}\|_\Omega\|\nabla(e_\phi^{n+1}+e_\phi^n)\|_\Omega+\frac{\tau}{\varepsilon}\|H^{n,n-1}\|_\Omega\|R_\phi^{n+\frac{1}{2}}\|_\Omega\\
&+A\tau^2\|\nabla R_\phi^{n+\frac{1}{2}}\|_\Omega\|\nabla(e_\phi^{n+1}-e_\phi^n)\|_\Omega\\
&+B_1\tau\|R_\phi^{n+\frac{1}{2}}\|_\Omega\|e_\phi^{n+1}-2e_\phi^n+e_\phi^{n-1}\|_\Omega+\tau\|R_\phi^{n+\frac{1}{2}}\|_\Omega\|R_\mu^{n+\frac{1}{2}}\|_\Omega\\
\leq&\frac{\varepsilon\tau}{2}\|\nabla R_\phi^{n+\frac{1}{2}}\|_\Omega^2+\frac{\varepsilon\tau}{4}\|\nabla e_\phi^{n+1}\|_\Omega^2+\frac{\varepsilon\tau}{4}\|\nabla e_\phi^n\|_\Omega^2+\frac{\tau}{2\varepsilon}\|H^{n,n-1}\|_\Omega^2\\
&+\frac{\tau}{2\varepsilon}\|R_\phi^{n+\frac{1}{2}}\|_\Omega^2+\frac{A\tau^2}{2}\|\nabla R_\phi^{n+\frac{1}{2}}\|_\Omega^2+\frac{A\tau^2}{2}\|\nabla(e_\phi^{n+1}-e_\phi^n)\|_\Omega^2+B_1\tau\|R_\phi^{n+\frac{1}{2}}\|_\Omega^2\\
&+\frac{B_1\tau}{2}\|e_\phi^{n+1}-e_\phi^n\|_\Omega^2+\frac{B_1\tau}{2}\|e_\phi^n-e_\phi^{n-1}\|_\Omega^2+\frac{\tau}{2}\|R_\phi^{n+\frac{1}{2}}\|_\Omega^2+\frac{\tau}{2}\|R_\mu^{n+\frac{1}{2}}\|_\Omega^2. \qquad (4.17)
\end{aligned}$$

For the second term of M_2, similar to the above estimate for the first term, we have

$$\begin{aligned}
&\tau(R_\psi^{n+\frac{1}{2}},e_\Gamma^{n+\frac{1}{2}})_\Gamma\\
\leq&\frac{\delta\kappa\tau}{2}\|\nabla_\Gamma R_\psi^{n+\frac{1}{2}}\|_\Gamma^2+\frac{\delta\kappa\tau}{4}\|\nabla_\Gamma e_\psi^{n+1}\|_\Gamma^2+\frac{\delta\kappa\tau}{4}\|\nabla_\Gamma e_\psi^n\|_\Gamma\\
&+\frac{\tau}{2\delta}\|\tilde{H}^{n,n-1}\|_\Gamma^2+\frac{\tau}{2\delta}\|R_\psi^{n+\frac{1}{2}}\|_\Gamma^2+\frac{A\tau^2}{2}\|\nabla_\Gamma R_\psi^{n+\frac{1}{2}}\|_\Gamma^2\\
&+\frac{A\tau^2}{2}\|\nabla_\Gamma(e_\psi^{n+1}-e_\psi^n)\|_\Gamma^2+B_2\tau\|R_\psi^{n+\frac{1}{2}}\|_\Gamma^2+\frac{B_2\tau}{2}\|e_\psi^{n+1}-e_\psi^n\|_\Gamma^2+\frac{B_2\tau}{2}\|e_\psi^n-e_\psi^{n-1}\|_\Gamma^2\\
&+\frac{\tau}{2}\|R_\psi^{n+\frac{1}{2}}\|_\Gamma^2+\frac{\tau}{2}\|R_\Gamma^{n+\frac{1}{2}}\|_\Gamma^2. \qquad (4.18)
\end{aligned}$$

Combining (4.17) and (4.18), we have

$$\begin{aligned}
&\tau(R_\phi^{n+\frac{1}{2}},e_\mu^{n+\frac{1}{2}})_\Omega+\tau(R_\psi^{n+\frac{1}{2}},e_\Gamma^{n+\frac{1}{2}})_\Gamma\\
\leq&C_5\tau^5+\frac{\varepsilon\tau}{4}\|\nabla e_\phi^{n+1}\|_\Omega^2+\frac{A\tau^2}{2}\|\nabla(e_\phi^{n+1}-e_\phi^n)\|_\Omega^2+\frac{\delta\kappa\tau}{4}\|\nabla_\Gamma e_\psi^{n+1}\|_\Gamma^2+\frac{A\tau^2}{2}\|\nabla_\Gamma(e_\psi^{n+1}-e_\psi^n)\|_\Gamma^2\\
&+\frac{B_1\tau}{2}\|e_\phi^{n+1}-e_\phi^n\|_\Omega^2+\frac{B_2\tau}{2}\|e_\psi^{n+1}-e_\psi^n\|_\Gamma^2+o(\tau^6), \qquad (4.19)
\end{aligned}$$

where $C_i(i=2,3,4,5)$ are constants independent of τ. We use the estimates for $H^{n,n-1}$, $\tilde{H}^{n,n-1}$ and the truncation terms $R_\phi^{n+\frac{1}{2}}$, $R_\psi^{n+\frac{1}{2}}$, $R_\mu^{n+\frac{1}{2}}$ and $R_\Gamma^{n+\frac{1}{2}}$ in Lemma 4.1. We also use the assumption that $\|e_\phi^n\|_\Omega$, $\|\nabla e_\phi^n\|_\Omega$, $\|e_\psi^n\|_\Gamma$, $\|\nabla_\Gamma e_\psi^n\|_\Gamma$ satisfy the Theorem 4.1. The fact that $\tau^2\leq\tau$, $o(\tau^6)$ is bounded and $R_\phi^{n+\frac{1}{2}}|_\Gamma=\gamma(R_\phi^{n+\frac{1}{2}})=R_\psi^{n+\frac{1}{2}}$ are also applied, where γ is the trace operator.

The term M_3 in (4.15) is estimated as follows.

$$\begin{aligned}&-\varepsilon\tau(\nabla e_\mu^{n+\frac{1}{2}},\nabla e_\phi^{n+1})_\Omega-\varepsilon\tau(\nabla_\Gamma e_\Gamma^{n+\frac{1}{2}},\nabla_\Gamma e_\psi^{n+1})_\Gamma\\ \le&2\varepsilon^2\tau\|\nabla e_\phi^{n+1}\|_\Omega^2+\frac{\tau}{8}\|\nabla e_\mu^{n+\frac{1}{2}}\|_\Omega^2+2\varepsilon^2\tau\|\nabla_\Gamma e_\psi^{n+1}\|_\Gamma^2+\frac{\tau}{8}\|\nabla_\Gamma e_\Gamma^{n+\frac{1}{2}}\|_\Gamma^2.\end{aligned}\tag{4.20}$$

For the first term of M_4 in (4.15), we have

$$\begin{aligned}&-\frac{1}{\varepsilon}\left(f\left(\frac{3}{2}\phi(t^n)-\frac{1}{2}\phi(t^{n-1})\right)-f\left(\frac{3}{2}\phi^n-\frac{1}{2}\phi^{n-1}\right),e_\phi^{n+1}-e_\phi^n\right)_\Omega\\ =&-\frac{\tau}{\varepsilon}\left(H^{n,n-1},\frac{e_\phi^{n+1}-e_\phi^n}{\tau}\right)_\Omega=-\frac{\tau}{\varepsilon}(H^{n,n-1},\Delta e_\mu^{n+\frac{1}{2}}+R_\phi^{n+\frac{1}{2}})_\Omega\\ \le&\frac{\tau}{\varepsilon}\|\nabla H^{n,n-1}\|_\Omega\|\nabla e_\mu^{n+\frac{1}{2}}\|_\Omega+\frac{\tau}{\varepsilon}\|H^{n,n-1}\|_\Gamma\|\partial_{\mathbf{n}}e_\mu^{n+\frac{1}{2}}\|_\Gamma+\frac{\tau}{\varepsilon}\|H^{n,n-1}\|_\Omega\|R_\phi^{n+\frac{1}{2}}\|_\Omega.\end{aligned}$$

By applying the trace theorem, we have

$$\begin{aligned}\|H^{n,n-1}\|_\Gamma=\|\gamma H^{n,n-1}\|_\Gamma\lesssim\|H^{n,n-1}\|_{H^1(\Omega)}&\lesssim\|H^{n,n-1}\|_\Omega+\|\nabla H^{n,n-1}\|_\Omega\\ &\lesssim\|e_\phi^n\|_\Omega+\|e_\phi^{n-1}\|_\Omega+\|\nabla e_\phi^n\|_\Omega+\|\nabla e_\phi^{n-1}\|_\Omega,\end{aligned}$$

where we use the assumption that e_ϕ^n satisfies the Theorem 4.1. So we obtain

$$\begin{aligned}&-\frac{1}{\varepsilon}(H^{n,n-1},e_\phi^{n+1}-e_\phi^n)_\Omega\\ \le&C_6\tau(\|e_\phi^n\|_\Omega+\|e_\phi^{n-1}\|_\Omega+\|\nabla e_\phi^n\|_\Omega+\|\nabla e_\phi^{n-1}\|_\Omega)\|\nabla e_\mu^{n+\frac{1}{2}}\|_\Omega\\ &+C_7\tau(\|e_\phi^n\|_\Omega+\|e_\phi^{n-1}\|_\Omega+\|\nabla e_\phi^n\|_\Omega+\|\nabla e_\phi^{n-1}\|_\Omega)\|\partial_{\mathbf{n}}e_\mu^{n+\frac{1}{2}}\|_\Omega\\ &+C_8\tau(\|e_\phi^n\|_\Omega+\|e_\phi^{n-1}\|_\Omega)\|R_\phi^{n+\frac{1}{2}}\|_\Omega\\ \le&C_9\tau^5+\frac{\tau}{4}\|\nabla e_\mu^{n+\frac{1}{2}}\|_\Omega^2+\frac{K\tau}{16}\|\partial_{\mathbf{n}}e_\mu^{n+\frac{1}{2}}\|_\Gamma^2.\end{aligned}\tag{4.21}$$

Here, $C_i\,(i=6,7,8,9)$ are constants independent of τ and we use the estimates for $H^{n,n-1}$ and R_ϕ^{n+1}.

For the second term of M_4, we have

$$\begin{aligned}&-(R_\mu^{n+\frac{1}{2}},e_\phi^{n+1}-e_\phi^n)_\Omega=-\tau\left(R_\mu^{n+\frac{1}{2}},\frac{e_\phi^{n+1}-e_\phi^n}{\tau}\right)_\Omega=-\tau(R_\mu^{n+\frac{1}{2}},\Delta e_\mu^{n+\frac{1}{2}}+R_\phi^{n+\frac{1}{2}})_\Omega\\ =&\tau(\nabla R_\mu^{n+\frac{1}{2}},\nabla e_\mu^{n+\frac{1}{2}})_\Omega-\tau(R_\mu^{n+\frac{1}{2}},\partial_{\mathbf{n}}e_\mu^{n+\frac{1}{2}})_\Gamma-\tau(R_\mu^{n+\frac{1}{2}},R_\phi^{n+\frac{1}{2}})_\Omega\\ \le&2\tau\|\nabla R_\mu^{n+\frac{1}{2}}\|_\Omega^2+\frac{\tau}{8}\|\nabla e_\mu^{n+\frac{1}{2}}\|_\Omega^2+\frac{8\tau}{K}\|R_\mu^{n+\frac{1}{2}}\|_\Gamma^2+\frac{K\tau}{32}\|\partial_{\mathbf{n}}e_\mu^{n+\frac{1}{2}}\|_\Gamma^2+\frac{\tau}{2}\|R_\mu^{n+\frac{1}{2}}\|_\Omega^2+\frac{\tau}{2}\|R_\phi^{n+\frac{1}{2}}\|_\Omega^2\\ \le&C_{10}\tau^5+\frac{\tau}{8}\|\nabla e_\mu^{n+\frac{1}{2}}\|_\Omega^2+\frac{K\tau}{32}\|\partial_{\mathbf{n}}e_\mu^{n+\frac{1}{2}}\|_\Gamma^2,\end{aligned}\tag{4.22}$$

where C_{10} is a constant independent of τ. Here, we apply the trace theorem that

$$\|R_\mu^{n+\frac{1}{2}}\|_\Gamma = \|\gamma R_\mu^{n+\frac{1}{2}}\|_\Gamma \lesssim \|R_\mu^{n+\frac{1}{2}}\|_{H^1(\Omega)} \lesssim \|R_\mu^{n+\frac{1}{2}}\|_\Omega + \|\nabla R_\mu^{n+\frac{1}{2}}\|_\Omega \lesssim \tau^2.$$

and use the estimates for $R_\mu^{n+\frac{1}{2}}$ and $R_\phi^{n+\frac{1}{2}}$.

Similarly, for the first term of M_5 in (4.15), we obtain

$$\begin{aligned}
&-\frac{1}{\delta}\left(g\left(\frac{3}{2}\psi(t^n)-\frac{1}{2}\psi(t^{n-1})\right)-g\left(\frac{3}{2}\psi^n-\frac{1}{2}\psi^{n-1}\right), e_\psi^{n+1}-e_\psi^n\right)_\Gamma \\
\le& C_{11}\tau^5+\frac{\tau}{4}\|\nabla_\Gamma e_\Gamma^{n+\frac{1}{2}}\|_\Gamma^2+\frac{K\tau}{32}\|\partial_{\mathbf{n}} e_\mu^{n+\frac{1}{2}}\|_\Gamma^2,
\end{aligned} \tag{4.23}$$

where C_{11} is a constant independent of τ. For the second term in M_5, we have

$$-(R_\Gamma^{n+\frac{1}{2}}, e_\psi^{n+1}-e_\psi^n)_\Gamma \le C_{12}\tau^5+\frac{\tau}{8}\|\nabla_\Gamma e_\Gamma^{n+\frac{1}{2}}\|_\Gamma^2+\frac{K\tau}{32}\|\partial_{\mathbf{n}} e_\mu^{n+\frac{1}{2}}\|_\Gamma^2, \tag{4.24}$$

where C_{12} is a constant independent of τ.

Combining the equations (4.15)-(4.24) leads to

$$\begin{aligned}
&\frac{\varepsilon}{2}(\|\nabla e_\phi^{n+1}\|_\Omega^2-\|\nabla e_\phi^n\|_\Omega^2)+\frac{\varepsilon}{2}(\|e_\phi^{n+1}\|_\Omega^2-\|e_\phi^n\|_\Omega^2+\|e_\phi^{n+1}-e_\phi^n\|_\Omega^2) \\
&+(A\tau-\frac{A\tau^2}{2})(\|\nabla e_\phi^{n+1}-\nabla e_\phi^n\|_\Omega^2+\|\nabla_\Gamma e_\psi^{n+1}-\nabla_\Gamma e_\psi^n\|_\Gamma^2) \\
&+\frac{B_1}{2}(\|e_\phi^{n+1}-e_\phi^n\|_\Omega^2-\|e_\phi^n-e_\phi^{n-1}\|_\Omega^2+\|e_\phi^{n+1}-2e_\phi^n-e_\phi^{n-1}\|_\Omega^2) \\
&+\frac{\delta\kappa}{2}(\|\nabla_\Gamma e_\psi^{n+1}\|_\Gamma^2-\|\nabla_\Gamma e_\psi^n\|_\Gamma^2)+\frac{\varepsilon}{2}(\|e_\psi^{n+1}\|_\Gamma^2-\|e_\psi^n\|_\Gamma^2+\|e_\psi^{n+1}-e_\psi^{n+1}\|_\Gamma^2) \\
&+\frac{B_2}{2}(\|e_\psi^{n+1}-e_\psi^n\|_\Gamma^2-\|e_\psi^n-e_\psi^{n-1}\|_\Gamma^2+\|e_\psi^{n+1}-2e_\psi^n-e_\psi^{n-1}\|_\Gamma^2) \\
&+\frac{\tau}{2}\|\nabla e_\mu^{n+\frac{1}{2}}\|_\Omega^2+\frac{\tau}{2}\|\nabla_\Gamma e_\Gamma^{n+\frac{1}{2}}\|_\Gamma^2+\frac{27K\tau}{36}\|\partial_{\mathbf{n}} e_\mu^{n+\frac{1}{2}}\|_\Gamma^2 \\
\le& C_{13}\tau^5+C_{14}\tau(\|\nabla e_\phi^{n+1}\|_\Omega^2+\|e_\phi^{n+1}\|_\Omega^2+\|e_\phi^{n+1}-e_\phi^n\|_\Omega^2 \\
&+\|\nabla_\Gamma e_\psi^{n+1}\|_\Gamma^2+\|e_\psi^{n+1}\|_\Gamma^2+\|e_\psi^{n+1}-e_\psi^n\|_\Gamma^2).
\end{aligned} \tag{4.25}$$

Here, C_{13} is a constant independent of τ and the constant $C_{14}=\max\{\frac{\varepsilon}{4}+2\varepsilon^2, \frac{\delta\kappa}{4}+2\varepsilon^2, \frac{B_1}{2}, \frac{B_2}{2}\}$, which is also independent of τ. Due to $\tau\le 1$, we have $A\tau-\frac{A\tau^2}{2}\ge 0$. By controlling the coefficients of Cauchy inequality, we can set the coefficient of term $\|\partial_{\mathbf{n}} e_\mu^{n+\frac{1}{2}}\|_\Gamma^2$ to be positive.

Summing (4.25) together for $n=0$ to m, we derive

$$
\begin{aligned}
&\frac{\varepsilon}{2}\|\nabla e_\phi^{m+1}\|_\Omega^2+\frac{\varepsilon}{2}\|e_\phi^{m+1}\|_\Omega^2+\frac{\delta\kappa}{2}\|\nabla_\Gamma e_\psi^{m+1}\|_\Gamma^2+\frac{\varepsilon}{2}\|e_\psi^{m+1}\|_\Gamma^2\\
&\quad+\frac{B_1}{2}\|e_\phi^{m+1}-e_\phi^m\|_\Omega^2+\frac{B_2}{2}\|e_\psi^{m+1}-e_\psi^m\|_\Gamma^2\\
&\quad+\sum_{n=0}^{m}\left(\frac{\varepsilon}{2}\|e_\phi^{n+1}-e_\phi^n\|_\Omega^2+\frac{\varepsilon}{2}\|e_\psi^{n+1}-e_\psi^n\|_\Gamma^2+\frac{B_1}{2}\|e_\phi^{n+1}-2e_\phi^n-e_\phi^{n-1}\|_\Omega^2+\frac{B_2}{2}\|e_\psi^{n+1}-2e_\psi^n-e_\psi^{n-1}\|_\Gamma^2\right.\\
&\qquad+\left(A\tau-\frac{A\tau^2}{2}\right)(\|\nabla e_\phi^{n+1}-\nabla e_\phi^n\|_\Omega^2+\|\nabla_\Gamma e_\psi^{n+1}-\nabla_\Gamma e_\psi^n\|_\Gamma^2)+\frac{\tau}{2}\|\nabla e_\mu^{n+\frac{1}{2}}\|_\Omega^2\\
&\qquad\left.+\frac{\tau}{2}\|\nabla_\Gamma e_\Gamma^{n+\frac{1}{2}}\|_\Gamma^2+\frac{27K\tau}{36}\|\partial_{\mathbf{n}} e_\mu^{n+\frac{1}{2}}\|_\Gamma^2\right)\\
&\le C_{13}(m+1)\tau^5+C_{14}\tau\sum_{n=0}^{m}(\|\nabla e_\phi^{n+1}\|_\Omega^2+\|e_\phi^{n+1}\|_\Omega^2\\
&\qquad+\|\nabla_\Gamma e_\psi^{n+1}\|_\Gamma^2+\|e_\psi^{n+1}\|_\Gamma^2+\|e_\phi^{n+1}-e_\phi^n\|_\Omega^2+\|e_\psi^{n+1}-e_\psi^n\|_\Gamma^2).
\end{aligned}
$$

Denote

$$
\omega=\min\left\{\frac{\varepsilon}{2},\frac{\delta\kappa}{2},\frac{B_1}{2},\frac{B_2}{2}\right\}, \tag{4.26}
$$

$$
\begin{aligned}
I_m=&\frac{\varepsilon}{2}\|\nabla e_\phi^{m+1}\|_\Omega^2+\frac{\varepsilon}{2}\|e_\phi^{m+1}\|_\Omega^2+\frac{\delta\kappa}{2}\|\nabla_\Gamma e_\psi^{n+1}\|_\Gamma^2+\frac{\varepsilon}{2}\|e_\psi^{m+1}\|_\Gamma^2\\
&+\frac{B_1}{2}\|e_\phi^{m+1}-e_\phi^m\|_\Omega^2+\frac{B_2}{2}\|e_\psi^{m+1}-e_\psi^m\|_\Gamma^2,
\end{aligned} \tag{4.27}
$$

$$
\begin{aligned}
S_m=&\sum_{n=0}^{m}\left(\frac{\varepsilon}{2}\|e_\phi^{n+1}-e_\phi^n\|_\Omega^2+\frac{\varepsilon}{2}\|e_\psi^{n+1}-e_\psi^n\|_\Gamma^2+\frac{B_1}{2}\|e_\phi^{n+1}-2e_\phi^n-e_\phi^{n-1}\|_\Omega^2\right.\\
&+\frac{B_2}{2}\|e_\psi^{n+1}-2e_\psi^n-e_\psi^{n-1}\|_\Gamma^2+\left(A\tau-\frac{A\tau^2}{2}\right)(\|\nabla e_\phi^{n+1}-\nabla e_\phi^n\|_\Omega^2+\|\nabla_\Gamma e_\psi^{n+1}-\nabla_\Gamma e_\psi^n\|_\Gamma^2)\\
&\left.+\frac{\tau}{2}\|\nabla e_\mu^{n+\frac{1}{2}}\|_\Omega^2+\frac{\tau}{2}\|\nabla_\Gamma e_\Gamma^{n+\frac{1}{2}}\|_\Gamma^2+\frac{27K\tau}{36}\|\partial_{\mathbf{n}} e_\mu^{n+\frac{1}{2}}\|_\Gamma^2\right).
\end{aligned}
$$

Then we have

$$
\begin{aligned}
I_m+S_m\le C_{13}(m+1)\tau^5+C_{14}\tau\sum_{n=0}^{m}&\left(\|\nabla e_\phi^{n+1}\|_\Omega^2+\|e_\phi^{n+1}\|_\Omega^2+\|\nabla_\Gamma e_\psi^{n+1}\|_\Gamma^2+\|e_\psi^{n+1}\|_\Gamma^2\right.\\
&\left.+\|e_\phi^{n+1}-e_\phi^n\|_\Omega^2+\|e_\psi^{n+1}-e_\psi^n\|_\Gamma^2\right)
\end{aligned}
$$

$$
\begin{aligned}
&= C_{13}T\tau^4 + \frac{C_{14}}{\omega}\tau\sum_{n=0}^{m}\omega\Bigg(\|\nabla e_\phi^{n+1}\|_\Omega^2 + \|e_\phi^{n+1}\|_\Omega^2 + \|\nabla_\Gamma e_\psi^{n+1}\|_\Gamma^2 + \|e_\psi^{n+1}\|_\Gamma^2 \\
&\quad + \|e_\phi^{n+1} - e_\phi^n\|_\Omega^2 + \|e_\psi^{n+1} - e_\psi^n\|_\Gamma^2\Bigg) \\
&\le C_{13}T\tau^4 + C_{15}\tau\sum_{n=0}^{m} I_n,
\end{aligned}
\tag{4.28}
$$

where $C_{15} = C_{14}/\omega$ is a constant independent of τ. By using the discrete Gronwall inequality, there exists some constants $\tilde{c}_0$, which is independent of τ, and $\tau_0 = 1/C_{18}$, such that, when $\tau < \tau_0$,

$$
I_m + S_m \le \tilde{c}_0\tau^2. \tag{4.29}
$$

This completes the proof. □

Remark 4.1. If we set the parameters as

$$
\varepsilon = \delta = 0.02, \quad \kappa = 1, \quad B_1 = B_2 = 50,
$$

then $C_{17} = \frac{B_1}{2} = 25$, $\omega = \frac{\varepsilon}{2} = 0.01$, so we have $C_{18} = 2500$ and $\tau_0 = 4\times 10^{-4}$. Namely, when $\tau < 4\times 10^{-4}$, the numerical results satisfy the second-order accuracy. Therefore, the error estimation can be applied in practice.

Remark 4.2. The error analysis of scheme (3.15)-(3.17) of GMS model (1.6) and scheme (3.18)-(3.21) of Liu-Wu model (1.7) are similar, and the proofs in detail are similar to the process of KLLM model Theorem 4.1.

Remark 4.3. The convergence analysis of the second-order scheme (3.1)-(3.6) of the KLLM model is inspired by the analysis of the first-order scheme in [3]. One of the differences is that we use the explicit extrapolation method for the nonlinear term f and g when proposing the second-order scheme. So we need the values of two time layers t^n and t^{n-1} when estimating $H^{n,n-1}$ in the proof, while in the first-order scheme, one only needs one time layer t^n. Another difference is that there exist two additional terms $(A\tau - \frac{A\tau^2}{2})(\|\nabla e_\phi^{n+1} - \nabla e_\phi^n\|_\Omega^2 + \|\nabla_\Gamma e_\psi^{n+1} - \nabla_\Gamma e_\psi^n\|_\Gamma^2)$ in the proof, since the stabilizers $-A\tau\Delta\left(\phi^{n+1} - \phi^n\right)$ and $-A\tau\Delta_\Gamma\left(\psi^{n+1} - \psi^n\right)$ are added in the second-order scheme to ensure the energy stability. However, we can guarantee that these terms are positive owing to $\tau \le 1$.

5 Numerical experiments

In this section, we present some numerical experiments of the Cahn-Hilliard model with different dynamic boundary conditions in two dimensions. For time discretization, we use the Crank-Nicolson scheme discussed in the previous sections. For spatial operators, we adopt the second-order central finite difference method to discretize them on a uniform spatial grid. For such a linear scheme, we use the generalized minimum residual method as the linear solver. We conduct the experiments on the rectangular domain $[0,1]^2$.

Example 1: Accuracy test

In this section, we first present the numerical accuracy tests of the scheme. The convergence rates of the proposed schemes (3.15)-(3.17), (3.18)-(3.21) and (3.1)-(3.6) are tested to support our error analysis, respectively. Let Ω be the unit square, the spatial step size $h=1/128$ and set the final time $T=4$. The time step $\tau=0.08,0.04,0.025,0.0125,0.01,0.005$. The parameters are set as $\varepsilon=\delta=0.02$, $\kappa=0.02$, $A=35$, $B_1=B_2=45$ for GMS model, $A=68$, $B_1=B_2=120$ for Liu-Wu model and $K=100$, $A=110$, $B_1=130$, $B_2=200$ for KLLM model. The initial data is taken as the piecewise constant setting:

$$\phi_0(x,y)=\begin{cases} 0, & x\in\Omega, \\ 1, & x\in\Gamma. \end{cases} \tag{5.1}$$

We choose F and G to be the modified double-well potential as

$$F(x)=G(x)=\begin{cases} (x-1)^2, & x>1, \\ \frac{1}{4}(x^2-1)^2, & -1\le x\le 1, \\ (x+1)^2, & x<-1. \end{cases}$$

Therefore, the second derivative of F with respect to ϕ and the second derivative of G with respect to ψ are bounded

$$\max_{\phi\in\mathbb{R}}|F''(\phi)|=\max_{\psi\in\mathbb{R}}|G''(\psi)|\le 2.$$

The errors are calculated as the differences between the solution of the coarse time step and that of the reference time step $\tau=2.5\times 10^{-4}$. In Fig. 1, we plot the sum of L^2 errors of ϕ and ψ between the numerical solution and the reference solution at final time with different time step sizes. The result shows clearly that the slope of fitting line is 2.131 for scheme (3.15)-(3.17) of GMS model, 2.044 for scheme (3.18)-(3.21) of Liu-Wu model and 2.157 for scheme (3.1)-(3.6) of KLLM model, which in turn verifies the convergence rates of the numerical schemes are all asymptotically at least second-order temporally for ϕ and ψ, which is consistent with our numerical analysis in Section 4.

Example 2: Shape deformation of a droplet

Here, we consider the shape deformation of a droplet. Initially, as the example in reference [3], a square droplet is placed in the area $[0,1]^2$ centered at $(0.5,0.25)$ and the length of each side is 0.5 (as shown in Fig. 2). The internal phase of the droplet is set to 1 and

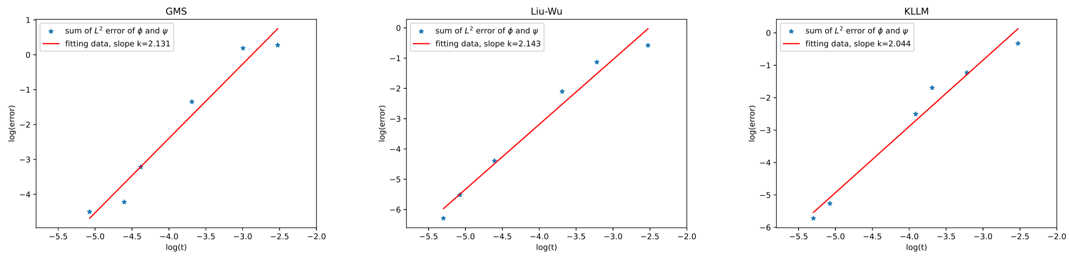

Figure 1: The numerical errors $\|e_\phi\|_\Omega+\|e_\psi\|_\Gamma$ at $T=4$ with different boundary conditions. Left: Boundary conditions of GMS. Middle: Boundary conditions of Liu-Wu. Right: Boundary conditions of KLLM.

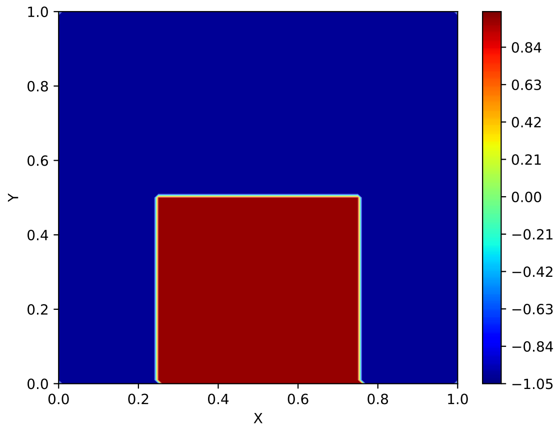

Figure 2: The initial data of the square shaped droplet.

the external phase is set to -1. The forms of F and G are taken as regular double-well potential functions (1.2). The parameters are set as $\varepsilon=\delta=0.02$. The stabilized parameters are chosen as $A=B_1=B_2=50$. We use the time step $\tau=4\times 10^{-4}$ and the spacial size $h=0.01$ to simulate the deformation of droplets from $t=0$ to $t=0.2$.

Fig. 3 shows the evolution process of GMS model (1.6) ($K=0$), Liu-Wu model (1.7) ($K=\infty$) and KLLM model (1.5) ($K=0.1,1,10$) with $\kappa=1$ respectively. The corresponding evolution of mass is plotted in Fig. 4. It can be seen that the square droplets are smoothed around the two upper corners of the initial structure of the three models. Then, with the increase of value of K, they tend to evolve into circular droplets with equal mean curvature. When $K<\infty$, the contact area increases and the bulk's mass of the droplet decreases. And the smaller K, the more mass exchanges between the interior and the boundary. In particular, when $K=\infty$ (for the Liu–Wu model), the bulk mass and the surface mass are conserved respectively. Under the constraint of mass conservation, the contact area between the droplet and the boundary almost keeps unchanged with time, which is consistent with the previous work [3,29].

The corresponding evolution of energy is plotted in Fig. 5. It is observed that our

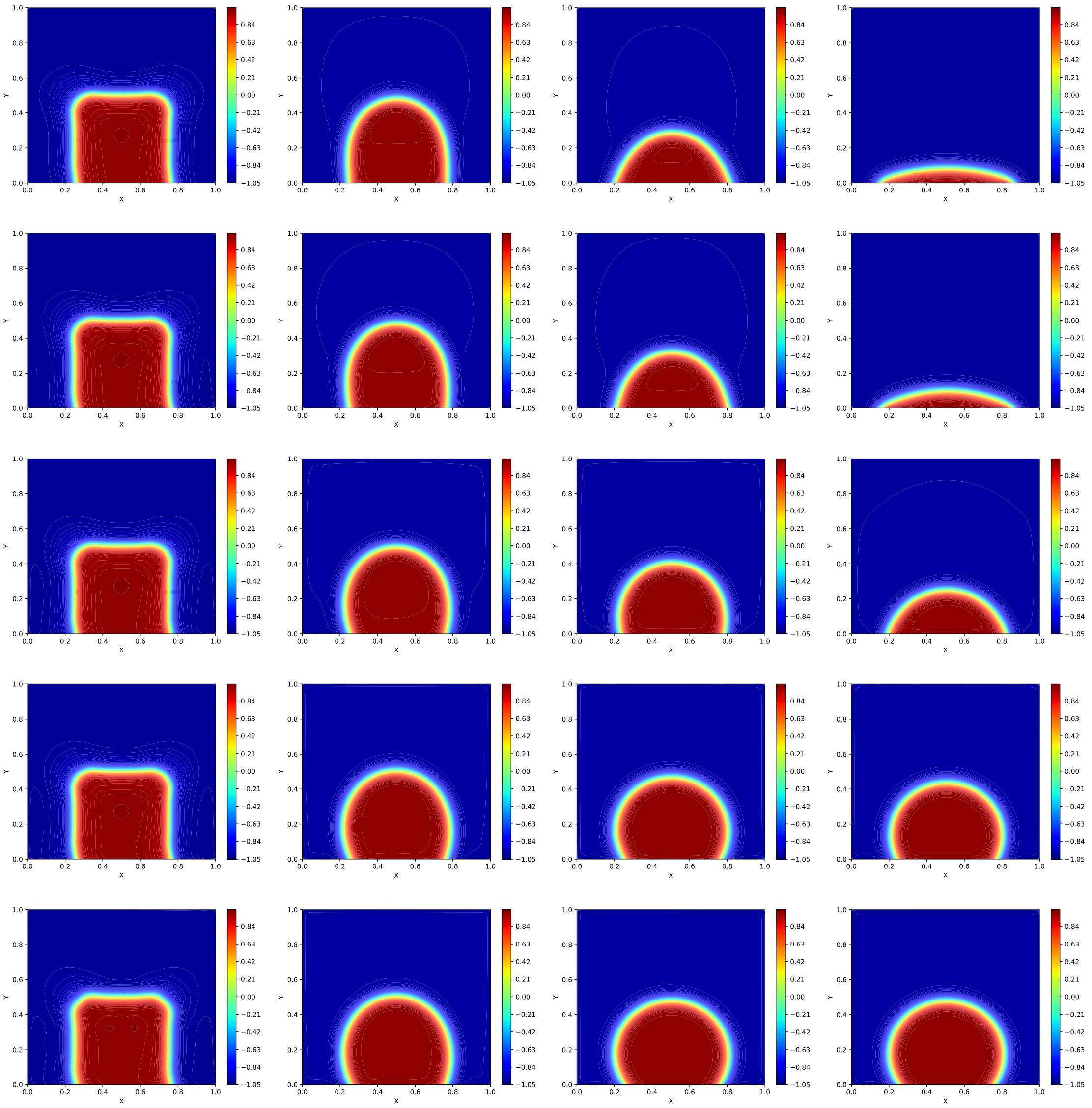

Figure 3: Phase-field at $t=0.001,0.01,0.08,0.2$. From top to bottom: $K=0,0.1,1,10,\infty$.

numerical schemes are energy stable. For different K, the initial energy decreases rapidly. We also find the decay rate depends on K largely. That is, the smaller K is, the faster the energy decreases.

Then, we check the experimental order of convergence (EOC) of ϕ and ψ for $K\to 0$ and $K\to\infty$ by using the droplet in the above as the initial data. The parameters are set as $\varepsilon=\delta=0.02$, $\kappa=1$, $A=B_1=B_2=50$, $\tau=2\times 10^{-4}$. We conduct numerical simulations from $t=0$ to $T=0.2$ with the spatial step size $h=0.01$. The following definitions are the same as work [3] (the last part of Section 5.3), which provides us with test criteria. Define

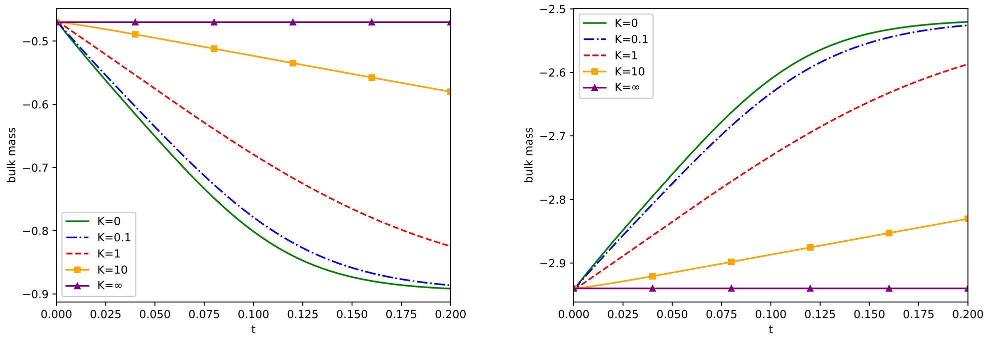

Figure 4: Time evolution of the bulk mass and the surface mass with different K with the initial data shown in Fig. 2.

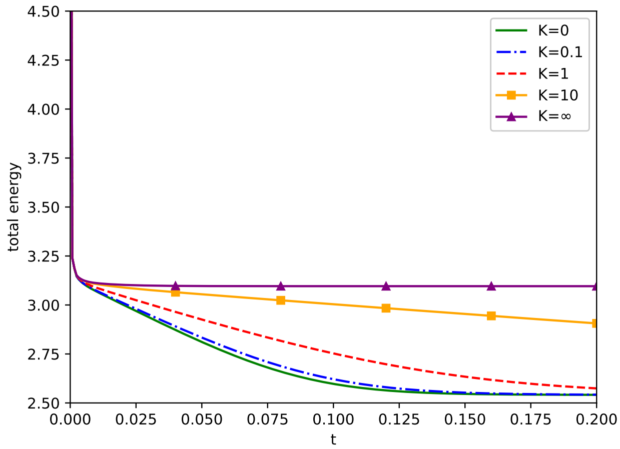

Figure 5: Time evolution of the total energy with different K with the initial data shown in Fig. 2.

$\phi_0^*(\psi_0^*)$ as the discrete solution under the case of $K=0$, $\phi_\infty^*(\psi_\infty^*)$ as the solution under the case of $K=\infty$ and $\phi_{K_i}(\psi_{K_i})$ as the solution under the case of K_i. We compare the discrete solutions $\phi_{K_i}(\psi_{K_i})$ with $\phi_0^*(\psi_0^*)$ for different K_i. The corresponding error is defined as

$$Err_{i,0}=\|\phi_{K_i}-\phi_0^*\|_{L^2(0,T;L^2(\Omega))} \quad \left(\text{or} \;\; \|\psi_{K_i}-\psi_0^*\|_{L^2(0,T;L^2(\Gamma))}\right),$$

where the time integral is approximated by the trapezoidal rule with time increment $\tilde{\tau}=10^{-3}$. The experimental order is defined as

$$Err_{K_i}=\frac{\ln\left(\frac{Err_{i+1,0}}{Err_{i,0}}\right)}{\ln\left(\frac{K_{i+1}}{K_i}\right)}.$$

Table 1: Comparison of ϕ for different K.

K	$\|\phi_{K_i}-\phi_0^*\|_{L^2(0,T;L^2(\Omega))}$	EOC	K	$\|\phi_{K_i}-\phi_\infty^*\|_{L^2(0,T;L^2(\Omega))}$	EOC
1E-4	3.96E-07	-	1E4	5.19E-04	-
2E-4	8.05E-07	1.0247	5E3	1.01E-02	-0.9999
5E-4	2.02E-06	1.0021	2.5E3	2.11E-03	-0.9996
1E-3	4.07E-06	1.0112	2E3	2.61E-03	-0.9994
0.01	4.58E-05	1.0514	1E3	5.21E-03	-0.9990
0.1	1.41E-03	1.4943	100	5.11E-02	-0.9934
1	1.61E-01	2.0518	10	3.81E-01	-0.8728

Table 2: Comparison of ψ for different K.

K	$\|\psi_{K_i}-\psi_0^*\|_{L^2(0,T;L^2(\Gamma))}$	EOC	K	$\|\psi_{K_i}-\psi_\infty^*\|_{L^2(0,T;L^2(\Gamma))}$	EOC
1E-4	1.31E-06	-	1E4	3.09E-04	-
2E-4	2.62E-06	1.0011	5E3	6.17E-04	-0.9998
5E-4	6.58E-06	1.0039	2.5E3	1.21E-03	-0.9995
1E-3	1.32E-05	1.9997	2E3	1.51E-03	-0.9992
0.01	1.29E-04	0.9921	1E3	3.11E-03	-0.9987
0.1	1.31E-03	0.9877	100	3.03E-02	-0.9929
1	9.33E-02	1.8716	10	2.53E-01	-0.9209

Similarly, we can define the corresponding error and the experimental order for the case of $K\to\infty$. The results for the convergence of ϕ and ψ are shown in Tables 1 and 2, indicating that for $K\leq 10^{-3}$ and $K\geq 10^3$, the convergence rate is almost 1. The second-order scheme also shows the same EOC as the first-order scheme [27], which validates our second-order scheme.

Example 3: Comparisons of the second-order scheme and the first-order scheme

In this section, we compare the second-order scheme with first-order results in [2]. We first take the droplet evolution as an example. The parameters are set as the same in Example 3. We set the time step size $\tau_1 = 1\times 10^{-4}$ for the first-order scheme and $\tau_2 = 2\times 10^{-4}$ for the second-order scheme. And the final time $T=0.2$. Note that we choose twice the time step size for second-order scheme. See Fig. 6 for the evolution of energy of the two experiments. We can see that the energy dissipation of second-order scheme is faster than the first-order scheme, but the stable states of the two tend to be consistent. In addition, the CPU time of the first-order and the second-order scheme at the final time $T=0.05$ are shown in Table 3, where we choose time step size $\tau_2=0.01$ for second-order scheme and $\tau_1=\tau_2^2$ for first-order scheme to maintain accuracy. The results reveal the second-order scheme is more efficient than the first-order scheme. That is, the CPU time

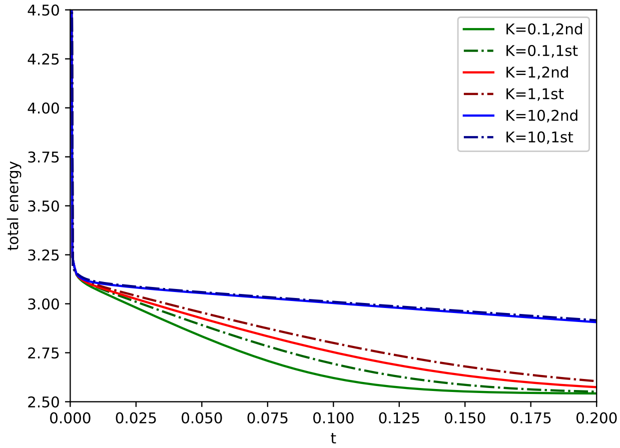

Figure 6: Time evolution of the total energy with first-order and second-order scheme with the initial data shown in Fig. 2.

Table 3: Comparison of CPU time (second) for first-order and second-order scheme with droplet as initial value.

K	0.1	1	10
1st	2.23E3	3.01E3	5.98E3
2nd	2.97E1	3.94E1	6.39E1

required by the first-order scheme is about 100 times that of the second-order scheme.

In the above experiments, we chose (1.2) as potential functions F and G. Another typical thermodynamically relevant example is the following logarithmic potential. Namely, for the bulk and surface potential, we consider the logarithmic Flory–Huggins potential as follows,

$$F(\phi)=\phi\ln\phi+(1-\phi)\ln(1-\phi)+\theta\phi\ln(1-\phi),$$
$$G(\psi)=\psi\ln\psi+(1-\psi)\ln(1-\psi)+\theta\psi\ln(1-\psi),$$

where the constant $\theta>0$. When the "shallow quenching" happens, the singular potential is often approximated by a polynomial of degree four like the double-well form (1.2) [44]. In this case, ϕ and ψ represent the mass concentration of one component in the bulk and on the boundary, so the corresponding physical correlation interval is $(0,1)$. One basic strategy is to regularize the singular potential in a suitable manner to ensure the logarithmic potential smooth enough [51]. Obviously, we don't need to worry about the overflow caused by any small fluctuation near the region boundary $(0,1)$ of the numerical solution.

Here, the time step $\tau=1\times10^{-4}$. The parameters are set as $\varepsilon=\delta=0.05,\kappa=1,\theta=2.5$. The artificial parameters $A=10,B_1=B_2=500$ are used to ensure that the scheme is

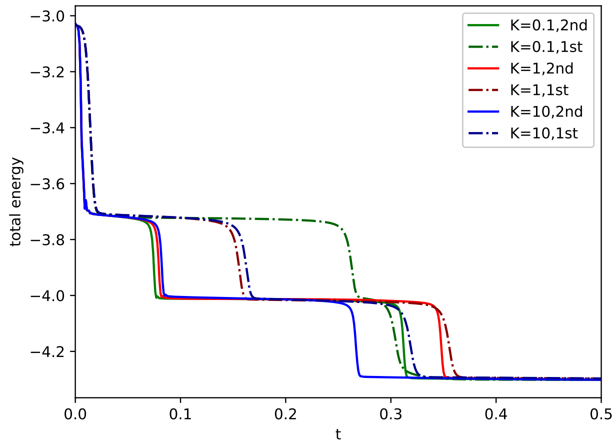

Figure 7: Time evolution of the total energy with different K with the initial data shown in Fig. 2.

Table 4: Comparison of CPU time (second) for first-order and second-order scheme with Flory–Huggins potential.

K	0.1	1	10
1st	1.92E3	2.86E3	3.23E3
2nd	4.04E1	1.02E2	6.84E2

stable. The initial data is set as random numbers between 0.4 and 0.6. Fig. 7 indicates the energy decreasing in steps with a quick decay at early stage and this quick decay behaviours more slowly with bigger K in second-order scheme but not obviously in first-order scheme. Besides, the energy of second-order scheme decreases faster than the first-order scheme. Similar to the previous experiment, we choose time step size $\tau_2 = 0.01$ for second-order scheme and $\tau_1 = \tau_2^2$ for first-order scheme to maintain accuracy. We compared CPU time of the two scheme running to final time $T = 0.05$ in Table 4. It's obvious that the second-order scheme save more CPU time than the first-order scheme.

To sum up, for the droplet model or the random scattering point as the initial value, with the double-well or the singular energy potential function, we both can obtain the efficiency of the second-order scheme.

6 Conclusions

We study the numerical algorithms and error analysis for the Cahn-Hilliard equation with dynamic boundary conditions. The second-order in time, linear and energy stable Crank-Nicolson scheme is proposed. We also present the corresponding proof of stability and convergence theoretically. In particular, to the best of our knowledge, we are the first to propose the second-order stabilized semi-implicit linear scheme for the KLLM model. Some numerical experiments are performed to verify the effectiveness and accuracy of the second-order numerical scheme, including the accuracy test, numerical simulations of three types of dynamic boundary conditions under various initial conditions and energy potential functions, the EOC of ϕ and ψ for $K \to 0$ and $K \to \infty$. By comparing with the first-order scheme, we can use the second-order scheme to reach the same state in less CPU time with different initial values and potential functions. Thus the efficiency of the second-order scheme is further verified.

Acknowledgments

Z.R. Zhang is partially supported by the NSFC Nos. 11871105 and 11231003. X.L. Bao is partially supported by the NSFC No. 12201050 and China Postdoctoral Science Foundation grant No. 2022M710425.

References

[1] F. Bai, D.Z. Han, X.M. He, and X.F. Yang. Deformation and coalescence of ferrodroplets in Rosensweig model using the phase field and modified level set approaches under uniform magnetic fields. *Commun. Nonlinear Sci. Numer. Simul.*, 85:105213, 2020.

[2] X.L. Bao and H. Zhang. Numerical approximations and error analysis of the Cahn-Hilliard equation with dynamic boundary conditions. *Commun. Math. Sci.*, 19(3):663–685, 2021.

[3] X.L. Bao and H. Zhang. Numerical approximations and error analysis of the Cahn-Hilliard equation with reaction rate dependent dynamic boundary conditions. *J. Sci. Comput.*, 87(3):1–32, 2021.

[4] P. Bates and P. Fife. The dynamics of nucleation for the Cahn-Hilliard equation. *SIAM J. Appl. Math.*, 53(4):990–1008, 1993.

[5] J.W. Cahn and J.E. Hilliard. Free energy of a nonuniform system. III. Nucleation in a two-component incompressible fluid. *J. Chem. Phys.*, 31(3):688–699, 1959.

[6] L.Q. Chen and J. Shen. Applications of semi-implicit Fourier-spectral method to phase field equations. *Comput. Phys. Commun.*, 108(2-3):147–158, 1998.

[7] L. Cherfils and M. Petcu. A numerical analysis of the Cahn-Hilliard equation with non-permeable walls. *Numer. Math.*, 128(3):517–549, 2014.

[8] L. Cherfils, M. Petcu, and M. Pierre. A numerical analysis of the Cahn-Hilliard equation with dynamic boundary conditions. *Discrete Contin. Dyn. Syst.*, 27(4):1511, 2010.

[9] P. Colli and T. Fukao. Cahn-Hilliard equation with dynamic boundary conditions and mass constraint on the boundary. *J. Math. Anal. Appl.*, 429(2):1190–1213, 2015.

[10] P. Colli, T. Fukao, and H. Wu. On a transmission problem for equation and dynamic boundary condition of Cahn-Hilliard type with nonsmooth potentials. *Math. Nachr.*, 293(11):2051–2081, 2020.

[11] P. Colli, G. Gilardi, R. Nakayashiki, and K. Shirakawa. A class of quasi-linear Allen-Cahn type equations with dynamic boundary conditions. *Nonlinear Anal.*, 158:32–59, 2017.

[12] Q. Du and X.B. Feng. The phase field method for geometric moving interfaces and their numerical approximations. *Handb. Numer. Anal.*, 21:425–508, 2020.

[13] X.L. Feng, T. Tang, and J. Yang. Stabilized Crank-Nicolson/Adams-Bashforth schemes for phase field models. *E. Asian. J. Appl. Math.*, 3(1):59–80, 2013.
[14] H.P. Fischer, P. Maass, and W. Dieterich. Novel surface modes in spinodal decomposition. *Phys. Rev. Lett.*, 79(5):893, 1997.
[15] T. Fukao, S. Yoshikawa, and S. Wada. Structure-preserving finite difference schemes for the Cahn-Hilliard equation with dynamic boundary conditions in the one-dimensional case. *Commun. Pur. Appl. Anal.*, 16(5):1915, 2017.
[16] C.G. Gal. A Cahn-Hilliard model in bounded domains with permeable walls. *Math. Method. Appl. Sci.*, 29(17):2009–2036, 2006.
[17] H. Garcke and P. Knopf. Weak solutions of the Cahn-Hilliard system with dynamic boundary conditions: A gradient flow approach. *SIAM J. Math. Anal.*, 52(1):340–369, 2020.
[18] H. Garcke, P. Knopf, and S. Yayla. Long-time dynamics of the Cahn-Hilliard equation with kinetic rate dependent dynamic boundary conditions. *Nonlinear Anal.*, 215:112619, 2022.
[19] G.R. Goldstein, A. Miranville, and G. Schimperna. A Cahn-Hilliard model in a domain with non-permeable walls. *Phys. D Nonlinear Phenom.*, 240(8):754–766, 2011.
[20] Y.Z. Gong, J. Zhao, and Q. Wang. Arbitrarily high-order linear energy stable schemes for gradient flow models. *J. Comput. Phys.*, 419:109610, 2020.
[21] G. Grun. On convergent schemes for diffuse interface models for two-phase flow of incompressible fluids with general mass densities. *SIAM J. Numer. Anal.*, 51(6):3036–3061, 2013.
[22] R. Guo, F. Filbet, and Y. Xu. Efficient high order semi-implicit time discretization and local discontinuous Galerkin methods for highly nonlinear PDEs. *J. Comput. Phys.*, 68(3):1029–1054, 2016.
[23] Y.N. He, Y.X. Liu, and T. Tang. On large time-stepping methods for the Cahn-Hilliard equation. *Appl. Numer. Math.*, 57(5-7):616–628, 2007.
[24] D. Jacqmin. Contact-line dynamics of a diffuse fluid interface. *J. Fluid Mech.*, 402:57–88, 2000.
[25] L.L. Ju, J. Zhang, and Q. Du. Fast and accurate algorithms for simulating coarsening dynamics of Cahn-Hilliard equations. *Comp. Mater. Sci.*, 108:272–282, 2015.
[26] P. Knopf and K.F. Lam. Convergence of a Robin boundary approximation for a Cahn-Hilliard system with dynamic boundary conditions. *Nonlinearity*, 33(8):4191, 2020.
[27] P. Knopf, K.F. Lam, C. Liu, and S. Metzger. Phase-field dynamics with transfer of materials: The Cahn-Hilliard equation with reaction rate dependent dynamic boundary conditions. *ESAIM Math. Model. Numer. Anal.*, 55(1):229–282, 2021.
[28] C. Liu and H. Wu. An energetic variational approach for the Cahn-Hilliard equation with dynamic boundary condition: Model derivation and mathematical analysis. *Arch. Ration. Mech. An.*, 233(1):167–247, 2019.
[29] X.J. Meng, X.L. Bao, and Z.R. Zhang. Second order stabilized semi-implicit scheme for the Cahn-Hilliard model with dynamic boundary conditions. *J. Comput. Appl. Math.*, 428:115145, 2023.
[30] X.J. Meng, Z.H. Qiao, C. Wang, and Z.R. Zhang. Artificial regularization parameter analysis for the no-slope-selection epitaxial thin film model. *CSIAM Trans. Appl. Math.*, 1(3):441–462, 2020.
[31] X.J. Meng and Z.R. Zhang. An adaptive BDF2 implicit time-stepping method for the no-slope-selection epitaxial thin film model. *Comput. Appl. Math.*, 42(3):124, 2023.
[32] R.M. Mininni, A. Miranville, and S. Romanelli. Higher-order Cahn-Hilliard equations with dynamic boundary conditions. *J. Math. Anal. Appl.*, 449(2):1321–1339, 2017.
[33] A. Novick-Cohen. *The Cahn–Hilliard equation. In: C. M. Dafermos and M. Pokorny (editors) Evolutionary Equations*. Handb. Differ. Eq., Vol. 4, Elsevier/North-Holland, 2008.

[34] R. Racke and S.M. Zheng. The Cahn-Hilliard equation with dynamic boundary conditions. *Adv. Differential Equ.*, 8(1):83–110, 2003.

[35] J. Shen, C. Wang, X.M. Wang, and S.M. Wise. Second-order convex splitting schemes for gradient flows with Ehrlich-Schwoebel type energy: Application to thin film epitaxy. *SIAM J. Numer. Anal.*, 50(1):105–125, 2012.

[36] J. Shen, J. Xu, and J. Yang. The scalar auxiliary variable (SAV) approach for gradient flows. *J. Comput. Phys.*, 353:407–416, 2018.

[37] J. Shen and X.F. Yang. Numerical approximations of Allen-Cahn and Cahn-Hilliard equations. *Discrete Contin. Dyn. Syst.*, 28(4):1669, 2010.

[38] J. Shen and X.F. Yang. The IEQ and SAV approaches and their extensions for a class of highly nonlinear gradient flow systems. *Contemp. Math*, 754:217–245, 2020.

[39] J. Shin, H.G. Lee, and J.Y. Lee. Unconditionally stable methods for gradient flow using convex splitting Runge-Kutta scheme. *J. Comput. Phys.*, 347:367–381, 2017.

[40] D. Trautwein. Finite-elemente approximation der Cahn-Hilliard-Gleichung mit Neumann- und dynamischen Randbedingungen. *Bachelor thesis, University of Regensburg*, 2018.

[41] J.X. Wang, K.J. Pan, and X.F. Yang. Convergence analysis of the fully discrete hybridizable discontinuous Galerkin method for the Allen-Cahn equation based on the invariant energy quadratization approach. *J. Sci. Comput.*, 91, 2022.

[42] L. Wang and H.J. Yu. Convergence analysis of an unconditionally energy stable linear Crank-Nicolson scheme for the Cahn-Hilliard equation. *J. Math. Study*, 51(1):89–114, 2018.

[43] L. Wang and H.J. Yu. On efficient second order stabilized semi-implicit schemes for the Cahn-Hilliard phase-field equation. *J. Sci. Comput.*, 77(2):1185–1209, 2018.

[44] H. Wu. A review on the Cahn-Hilliard equation: Classical results and recent advances in dynamic boundary conditions. *Electronic Research Archive*, 30(8):2788–2832, 2022.

[45] X. Wu, G.J. Van Zwieten, and K.G. Van der Zee. Stabilized second-order convex splitting schemes for Cahn-Hilliard models with application to diffuse-interface tumor-growth models. *Int. J. Numer. Meth. Bio.*, 30(2):180–203, 2014.

[46] Z. Xu, X.F. Yang, H. Zhang, and Z.Q. Xie. Efficient and linear schemes for anisotropic Cahn-Hilliard model using the stabilized-invariant energy quadratization (S-IEQ) approach. *Comput. Phys. Commun.*, 238:36–49, 2019.

[47] X.F. Yang. Linear, first and second-order, unconditionally energy stable numerical schemes for the phase field model of homopolymer blends. *J. Comput. Phys.*, 327:294–316, 2016.

[48] X.F. Yang, Z.L. Cui, M.G. Forest, Q. Wang, and J. Shen. Dimensional robustness and instability of sheared, semidilute, nanorod dispersions. *Multiscale Model. Simul.*, 7(2):622–654, 2008.

[49] X.F. Yang and H.J. Yu. Efficient second order unconditionally stable schemes for a phase field moving contact line model using an invariant energy quadratization approach. *SIAM J. Sci. Comput.*, 40(3):B889–B914, 2018.

[50] X.F. Yang and G.D. Zhang. Convergence analysis for the invariant energy quadratization (IEQ) schemes for solving the Cahn-Hilliard and Allen-Cahn equations with general nonlinear potential. *J. Sci. Comput.*, 82(3):1–28, 2020.

[51] X.F. Yang and J. Zhao. On linear and unconditionally energy stable algorithms for variable mobility Cahn-Hilliard type equation with logarithmic Flory-Huggins potential. *Commun. Comput. Phys.*, 25(3):703–728, 2019.

[52] X.F. Yang, J. Zhao, and X.M. He. Linear, second order and unconditionally energy stable schemes for the viscous Cahn-Hilliard equation with hyperbolic relaxation using the invariant energy quadratization method. *J. Comput. Appl. Math.*, 343:80–97, 2018.

[53] J. Zhang and X.F. Yang. A new magnetic-coupled Cahn-Hilliard phase-field model for diblock copolymers and its numerical approximations. *Appl. Math. Lett.*, 107:106412, 2020.

[54] J. Zhao, X.F. Yang, Y.Z. Gong, X.P. Zhao, X.G. Yang, J. Li, and Q. Wang. A general strategy for numerical approximations of non-equilibrium models-part I: Thermodynamical systems. *Int. J. Numer. Anal. Mod.*, 15(6):884–918, 2018.